



Shah, Tanushree (2023) *Classification of tight contact structures on some Seifert fibred manifolds with four exceptional fibres*. PhD thesis.

<https://theses.gla.ac.uk/83486/>

Copyright and moral rights for this work are retained by the author

A copy can be downloaded for personal non-commercial research or study, without prior permission or charge

This work cannot be reproduced or quoted extensively from without first obtaining permission in writing from the author

The content must not be changed in any way or sold commercially in any format or medium without the formal permission of the author

When referring to this work, full bibliographic details including the author, title, awarding institution and date of the thesis must be given

Enlighten: Theses

<https://theses.gla.ac.uk/>
research-enlighten@glasgow.ac.uk

Classification of tight contact structures on some Seifert fibred manifolds with four exceptional fibres

by
Tanushree Shah

A thesis submitted in fulfillment of the requirements
for the degree of

Doctor of Philosophy

at the

School of Mathematics & Statistics
College of Science & Engineering
University of Glasgow



Author's declaration

I declare that, except where explicit reference is made to the contribution of others, this dissertation is the result of my own work and has not been submitted for any other degree at the University of Glasgow or any other institution.

Acknowledgements

This thesis is a culmination of my research and discovery in the relatively unknown world of contact topology. There is a long list of people and institutions instrumental in making my dream a reality, and I am eternally grateful to all of them throughout this journey. Some deserve a special mention: Brendan, Ana, and Andy: thank you for inspiring, encouraging, and supporting me. I cannot understate how pivotal your guidance has been in making sure I stay the course. I never thought I could go this further so thank you for pushing me! The University of Glasgow: for all the warmth, love and unfailing magic that your world has created. This charming campus with its historic halls will forever hold a place in my heart. How could someone not feel special working here!?! My peers at the Dept of Mathematics: I know you're all grinning and winking right now but you know as well as I do that my research would have been a monumental challenge without all the memes, games, gifts, outings and banter in the break room. You folks are the best! I'll always remain grateful for the loops of frequent feedback and technical wisdom I received from Lisa, Irena and Radha - my peers and the best of friends be it math or magic! Sending lots of love to my Glasgow family - Sania, Sonali and Vaibhav - who made me feel right at home all these years. Finally, my family - mummy, papa, Himu, Kartik and Rita: you egged me on during my ebbs and flows, knowing full well that they would occur but also knowing that I would emerge stronger with all the tough love you gave me! I would like to virtually dedicate a heartfelt shout-out to everyone I crossed paths with that provided wisdom and courage, and helped me move that needle in the right direction. To all of them: "know this: you deserve credit for this document too". Finally and importantly, I am grateful to the College of Science and Engineering at the University of Glasgow for its College Scholarship which enabled my research during these years.

Dedication

To the rejoicing flame of light.

List of Figures

2.1	Standard contact structure on \mathbb{R}^3 [Pat].	6
2.2	Overtwisted disk [Pat].	6
2.3	Examples of front projection of Legendrian knots [Etn].	8
2.4	Legendrian Reidemeister moves [Etn].	8
2.5	Right-handed crossings (right) contribute +1 to the writhe while left-handed crossings (left) contribute -1.	9
2.6	Downward and upward cusps.	10
2.7	Calculation of Thurston-Bennequin number and rotation number [Hon].	10
3.1	Elliptic and hyperbolic singularities [Hon].	14
3.2	Characteristic foliation on unit sphere in \mathbb{R}^3 [Pat].	14
3.3	Contact structure on T^3 [Pat].	15
3.4	Characteristic foliation on $x = \text{constant}$ in T^3 [Pat].	15
3.5	Characteristic foliation on $z = \text{constant}$ in T^3 [Pat].	16
3.6	Characteristic foliation near the dividing set Γ_Σ [Pat].	18
3.7	The dashed lines are the dividing set for the torus $x = \text{constant}$ [Pat].	19
3.8	Bypass [GS].	22
3.9	Dividing curves before and after bypass attachment [Hon1].	23
3.10	Bypass attachment on torus [Hon1].	24
3.11	Farey tessellation of hyperbolic disk [Hon1].	25
3.12	Arc in Farey tessellation from -2 to 0 [Hon1].	26
4.1	Surgery description of the Seifert manifold.	33
4.2	Legendrian realisation of unknot with Thurston-Bennequin number -1.	33
4.3	Legendrian realisations of the unknot with Thurston-Bennequin number -3.	33
4.4	Decomposition of a Seifert fibred 3-manifold with four exceptional fibres.	34
4.5	Dividing curve on Σ with contact structure ξ_A on $\Sigma \times S^1$	37
4.6	Σ and Σ' with their boundary slopes.	37

4.7	Possible dividing curves on pair of pants.	38
4.8	Dividing curves on boundary of $\Sigma' \times I$	40
4.9	Possible dividing set on Σ	40
4.10	Two possibilities of dividing curves on \mathbb{D}^2 with $t(\partial\mathbb{D}) = 2$ [Hon1].	41
4.11	Possible dividing set on Σ	41
4.12	Positive (left) and Negative (right) sign configuration of dividing sets on A_2 and A_1	42
4.13	Dividing set of ξ_B on Σ	43
4.14	Dividing set of $\xi_{B'}$ on Σ	43
4.15	Dividing set of ξ_C and ξ_D on Σ	44
4.16	Dividing set of $\xi_{C'}$ and $\xi_{D'}$ on Σ	45
4.17	Four possible configurations of dividing curves on Σ	45
4.18	Dividing set of $\xi_{E'}$ on Σ	46
4.19	Dividing curve configurations on the sphere with four holes representing all possible tight contact structures on Y	47
4.20	Dividing curve configuration on the sphere with four holes.	48
4.21	Surgery diagram representations of the manifold $M(0; -q_1/p_1, -q_2/p_2, -q_3/p_3, -q_4/p_4)$	49
4.22	Decomposition of Y	51
4.23	Different sections of a tight contact structures on $\{\text{shirt}\} \times S^1$	52

Contents

1	Introduction	1
2	Contact structures	5
2.1	Legendrian knots	7
2.2	Legendrian surgery	10
3	Convex surface theory	13
3.1	Dividing set	16
3.1.1	Giroux’s flexibility and Giroux’s criterion	18
3.1.2	Legendrian realisation	20
3.1.3	Twisting	21
3.2	Bypasses	21
3.3	Classification of tight contact structures on basic blocks	26
3.3.1	Flexibility of the characteristic foliations	26
3.3.2	Standard neighbourhood of Legendrian curve	27
3.3.3	Basic slices	28
3.3.4	Classification of tight contact structures on $T^2 \times I$	28
3.3.5	Giroux torsion	29
4	Tight structures on Seifert manifolds	31
4.1	Seifert fibred 3-manifolds	31
4.2	An example case	32
4.2.1	Upper bound	34
4.2.2	Maximising twisting numbers	35
4.2.3	Combining tight contact structures on basic blocks	36
4.3	General case	48
4.4	Concluding remarks	53

Chapter 1

Introduction

Contact topology was born from the work of Huygens, Hamilton and Jacobi on geometric optics over two centuries ago [Etn]. It has witnessed remarkable breakthroughs recently, resulting in a coherent holistic picture of this field. This development further evolved into a subtle relationship between contact structures, and 3 and 4 dimensional topology [Etn]. More specifically, there is a one-to-one correspondence between open book decompositions and contact structures in 3-dimensions defined by Giroux's fundamental theorem [Gir1].

Jean Martinet showed that any oriented closed 3-manifold admits a contact structure [JM]. The dichotomy between tight and overtwisted contact structures was first discovered by Bennequin [B]. Eliashberg proved that there is an equivalence between overtwisted contact structures and homotopy classes of tangent planes on a 3-manifold [Eli].

Eliashberg classified tight contact structures on S^3 and \mathbb{R}^3 . Kanda [Kan] and Giroux [Gir1] (independently) gave classifications on the 3-torus. Etnyre [Et1] classified tight contact structures on some lens spaces. Honda gave a complete classification of tight contact structures on lens spaces, solid tori, and toric annuli with convex boundary [Hon1] and a complete classification results for tight contact structures on torus bundles which fibre over the circle, and circle bundles which fibre over closed surfaces [Hon2]. The classification for almost all of these manifolds was also proven by Giroux in [Gir3]. Etnyre and Honda show the non-existence of contact structures on some Seifert fibered manifolds in [EH]. Ghiggini and Shönenberger gave the first classification with a non-zero number of tight contact structures on some small Seifert fibered spaces. Hao Wu gave the classification on small Seifert fibred spaces with $e_0 \neq 0, -1, -2$. Classification on some of the remaining Seifert fibred manifolds is given by Ghiggini [G], Ghiggini, Lisca and Stipicz [GLS1, GLS2], Matkovič [M]. Jonathan Simone gave a classification of tight contact structures on some plumbed 3-manifolds [Sim].

We build on some of the above results. We classify tight contact structures on some Seifert fibred manifolds with four exceptional fibres with zero Giroux torsion. For the Seifert fibred manifold $M(g; q_1/p_1, \dots, q_4/p_4)$, where g is the genus of the base surface B , we define the *Euler number*, $e_0(M) = \lfloor \frac{-q_1}{p_1} \rfloor + \lfloor \frac{-q_2}{p_2} \rfloor + \lfloor \frac{-q_3}{p_3} \rfloor + \lfloor \frac{-q_4}{p_4} \rfloor$, where $\lfloor x \rfloor$ is the greatest integer not greater than x . We denote the continued fraction expansion of $\frac{-q_i}{p_i}$ by $[a_0^i, a_1^i, \dots, a_{m_i}^i]$. We first look at an example case in detail before proving the general result. We look at the tight contact structures on $M(0; -1/2, -1/2, -1/2, -1/2)$ which has $e_o = -4$.

Theorem 1.1. *There are three tight contact structures on $M(0; -1/2, -1/2, -1/2, -1/2)$ without Giroux torsion up to contact isotopy. All three of them are Stein fillable. For each $n \in \mathbb{Z}^+$ there exists at least one tight contact structure with n -Giroux torsion on M . These tight contact structures are not weakly fillable.*

Once we have calculated the tight contact structures on this example case, it is computationally easy to generalise to manifolds $M = M(0; -q_1/p_1, -q_2/p_2, -q_3/p_3, -q_4/p_4)$ with $e_0(M) \leq -4$.

Theorem 1.2. *Let $M = M(0; -q_1/p_1, -q_2/p_2, -q_3/p_3, -q_4/p_4)$ where $e_0 \leq -4$ and $p_i, q_i \in \mathbb{Z}$ with, $p_i \geq 2$, $q_i \geq 1$ and $\gcd(p_i, q_i) = 1$. On M there are exactly $|(e_0(M) + 1)\prod_{i=1}^4 \prod_{j=1}^{m_i} (a_j^i + 1)|$ tight contact structures with zero Giroux torsion up to contact isotopy. All of these can be constructed by Legendrian -1 surgery and hence are Stein fillable. For each $n \in \mathbb{Z}^+$ there exists at least one tight contact structure with n -Giroux torsion on M . These tight contact structures are not weakly fillable.*

Chapter 2 is an introduction to contact structures. We start looking at definitions, examples and different notions of equivalence of contact structures. Contact structures come in two flavours: tight or overtwisted. The classification of overtwisted contact structures is well understood, as opposed to that of tight contact structures. We get the classification of tight contact structures by giving a lower bound and upper bound to the number of tight contact structures on a manifold M and then showing that the two bounds match. Chapter 2 focuses on the theory we need to get the lower bound. We study the construction of tight contact structures via Legendrian surgery. To understand this surgery we need to study Legendrian knots and links with their invariants, Thurston-Bennequin number and rotation number. Some of the tight contact structures we get by surgery might be isotopic. To distinguish non-isotopic contact structures we use Lisca-Matić's result [LM], which uses Chern numbers and Stein structures.

Chapter 3 explains convex surface theory. We present results on characteristic foliations, sets of dividing curves and bypasses in a contact manifold which help us to get the upper bound on the number of tight contact structures. Then we look at a couple of classification theorems that we use to classify tight contact structures on our Seifert fibred manifolds.

We give the proofs of Theorems 1.1 and 1.2 in Chapter 4. We start by constructing our Seifert fibred manifolds. Then we use methods from Chapter 2 to get the lower bound and methods from Chapter 3 to obtain the upper bound on the number of tight contact structures with zero Giroux torsion. These two numbers match and therefore we obtain a classification result.

It came to the author's notice 6 months before submission that Elif Medetogullari had similar results which were never published.

Chapter 2

Contact structures

In this chapter, we provide a brief introduction to contact structures on 3-manifolds, followed by a review of the overtwisted and tight dichotomy, and the classification of overtwisted contact structures. In Section 2.1, we review the concept of Legendrian knots and their invariants. In Section 2.2, we recall Legendrian surgery and collect important results. We start by looking at the definition and examples of contact structures. The main references for this chapter are [Etn],[Hon],[Eli1],[Eli2].

A plane field ξ on a 3-manifold M is called a *contact structure* if there exists a 1-form α such that $\xi = \ker(\alpha)$ and $\alpha \wedge d\alpha \neq 0$.

Now we will look at two contact structures on \mathbb{R}^3 . Both examples are from [Etn]. These two examples illustrate two different types of contact structure. As we will see, these two types are exclusive of each other. This dichotomy is very helpful in understanding and classifying contact structures.

Consider the manifold \mathbb{R}^3 with standard Cartesian coordinates (x, y, z) and 1-form $\alpha = dz + xdy$. In particular $d\alpha = dx \wedge dy$. Hence $\alpha \wedge d\alpha = dx \wedge dy \wedge dz \neq 0$. Hence $\ker(\alpha)$ defines a contact structure. This contact structure is spanned by $(\partial/\partial x, x\partial/\partial z - \partial/\partial y)$. On the $x = 0$ plane, the contact planes are spanned by $(\partial/\partial x, \partial/\partial y)$ hence they are horizontal. At $x = 1$ the contact planes are spanned by $(\partial/\partial x, \partial/\partial z - \partial/\partial y)$. Hence the planes are rotated by 45° . As we go along the x -axis, the planes rotate clockwise in the positive x direction and anticlockwise in the negative x direction. The planes become more and more vertical as we approach $x = \infty$. Along the z -axis and the y -axis there is no rotation. This plane field is called the standard contact structure, ξ_{std} , on \mathbb{R}^3 . In Figure 2.1 we are looking at the plane $z = 0$.

On \mathbb{R}^3 with (r, θ, z) coordinates, consider the 1-form $\cos(r)dz + r \sin(r)d\theta$. Pick a ray perpendicular to the z -axis in the $z = 0$ plane. The contact planes are horizontal at the origin and when $r = k\pi$ for each $k \in \mathbb{Z}$. They rotate anti-clockwise as we go along

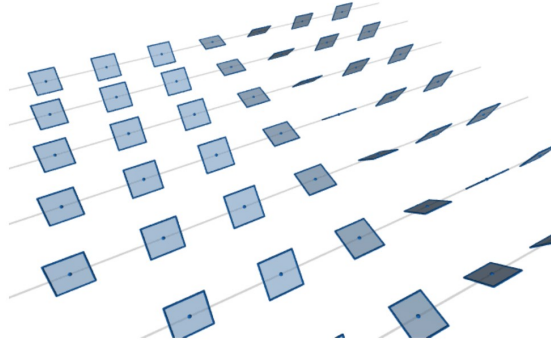


Figure 2.1: Standard contact structure on \mathbb{R}^3 [Pat].

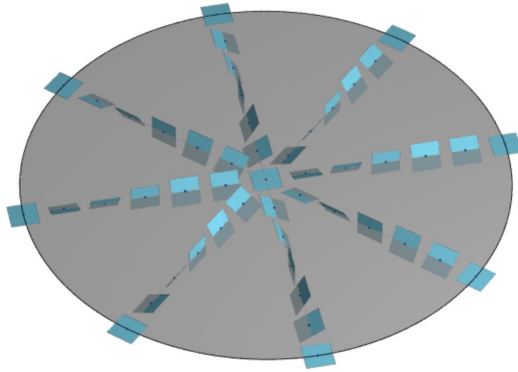


Figure 2.2: Overtwisted disk [Pat].

our ray. Figure 2.2 shows a disk of radius π on the $z = 0$ plane. Notice that the tangent space of the disk agrees with the contact structure planes along the boundary.

A contact manifold is *overtwisted* if it contains an embedded disk where the contact structure is tangent to the disk on the boundary, as shown in Figure 2.2. A contact structure that is not overtwisted is called *tight*.

Two contact structures ξ_0 and ξ_1 on M are *contactomorphic* if there exists a diffeomorphism $f : M \rightarrow M$ such that $f_*(\xi_0) = \xi_1$. The two examples above are not contactomorphic. The standard contact structure on \mathbb{R}^3 is tight, and the example above is overtwisted.

There are other notions of equivalence of contact structures which we will be using. Two contact structures on a 3-manifold are called *homotopic* if they are homotopic as tangent plane distributions. They are called *isotopic* if there is a homotopy between

them through contact structures. Note that isotopy is a stricter condition than contact isotopy.

Notice that in the standard contact structure on \mathbb{R}^3 , the contact planes become vertical at infinity. This gives us the standard contact structures on \mathbb{S}^3 , when we look at \mathbb{S}^3 as the one-point compactification of \mathbb{R}^3 .

The following theorem by Eliashberg classifies all overtwisted contact structures on a 3-manifold M .

Theorem 2.1 (Eliashberg [Eli]). *Let M be an oriented connected 3-manifold. Let us fix a point $p \in M$ and an embedded disk centred at the point p . Let $\text{Distr}(M)$ denote the space of all tangent 2-plane distributions on M fixed at the point p . Let $\text{Cont}^{\text{ot}}(M)$ denote the subspace of $\text{Distr}(M)$ which consists of all overtwisted contact structures which have the standard overtwisted disk centered at p . The inclusion from $\text{Cont}^{\text{ot}}(M)$ into $\text{Distr}(M)$ is a homotopy equivalence.*

Theorem 2.1 implies Theorem 2.2 but the other way round is not true. Since Theorem 2.2 is clearer and more concise it is often stated as the classification theorem for overtwisted contact structures.

Theorem 2.2 (Eliashberg [Eli]). *Given a closed 3-manifold M , let \mathcal{H} be the set of homotopy classes of (oriented) plane fields on M and let \mathcal{C} be the set of isotopy classes of (oriented) overtwisted contact structures on M . The natural inclusion map from \mathcal{C} to \mathcal{H} induces a bijection.*

The classification of overtwisted contact structures is very well understood, as opposed to that of tight contact structures as we will see later in Section 2.2.

2.1 Legendrian knots

In this section, we will look at knots embedded in \mathbb{R}^3 with the standard contact structure ξ_{std} , which is given as $\ker(dz + xdy)$, and some invariants of these knots. For details on this section we refer to [Etn].

A knot γ in $(\mathbb{R}^3, \xi_{\text{std}})$ is called a *Legendrian knot* if γ is tangent to ξ_{std} at every point.

To picture γ , we project it onto the yz -plane. We call this projection the front projection of γ . As we have seen in the example earlier, the contact planes become vertical only at infinity; so, there are no vertical tangencies in the front projection. Since a Legendrian knot in \mathbb{R}^3 is tangent to the contact planes given as $\ker(dz + xdy)$, the x -coordinate of γ is given by (minus) the slope in the front projection. In every

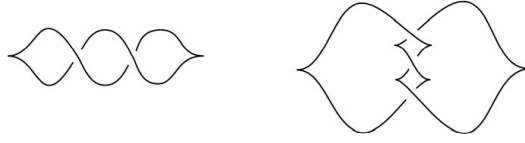


Figure 2.3: Examples of front projection of Legendrian knots [Etn].

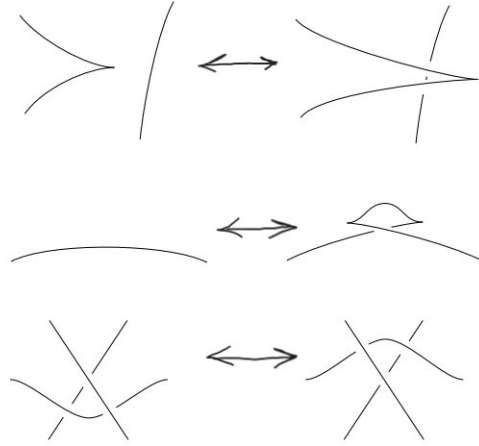


Figure 2.4: Legendrian Reidemeister moves [Etn].

crossing, the strands of γ with the smaller slopes lie in front of the strands with the larger slope. Figure 2.3 shows two examples. The first one is an unknot and the second one is a trefoil.

Two Legendrian knots γ_1 and γ_2 are *Legendrian isotopic* if there is a smooth map $\Phi : S^1 \times [0, 1] \rightarrow \mathbb{R}^3$ so that $\Phi(S^1, 0) = \gamma_0$, $\Phi(S^1, 1) = \gamma_1$ and $\Phi(S^1, t) = \gamma_t$ are embedded Legendrian knots. One can prove that two Legendrian knots γ_0 and γ_1 are Legendrian isotopic if and only if there is a 1-parameter family of contact diffeomorphisms $\phi_t : \mathbb{R}^3 \rightarrow \mathbb{R}^3$ such that $\phi_0 = id$ and $\phi_1(\gamma_0) = \gamma_1$. We look at Legendrian knots up to Legendrian isotopy. Two Legendrian knots are Legendrian isotopic if and only if one can go from one front projection to the other by Legendrian Reidemeister moves. These moves are shown in Figure 2.4.

Now let us look at some invariants of Legendrian knots. Let γ be an oriented Legendrian knot in $(\mathbb{R}^3, \xi_{std})$. Consider a vector field v along γ that is transverse to ξ_{std} . Using this we can get a knot γ' by pushing γ in the direction of v . The *Thurston-Bennequin* invariant of γ , $tb(\gamma)$ is the linking number of γ and γ' .

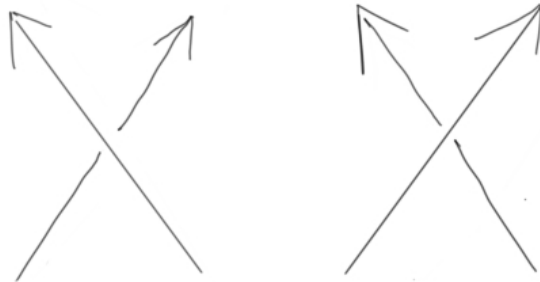


Figure 2.5: Right-handed crossings (right) contribute $+1$ to the writhe while left-handed crossings (left) contribute -1 .

Let Σ be a Seifert surface for γ , oriented in such a way that the given orientation of γ matches its orientation as the boundary of Σ . Since Σ is a surface with boundary, we can choose a trivialisation $\xi|_{\Sigma} = \Sigma \times \mathbb{R}^2$ and let $\pi : \xi|_{\Sigma} \rightarrow \mathbb{R}^2$ be the projection onto \mathbb{R}^2 factor. Let $f : S^1 \rightarrow \gamma \subset \mathbb{R}^3$ be a (regular) parametrisation of γ compatible with its orientation. The *rotation number* with respect to Σ , $r(\gamma, \Sigma)$, is the degree of the map $\pi \circ f' : S^1 \rightarrow \mathbb{R}^2 \setminus \{0\}$. Note that the rotation number does not depend on the choice of trivialisation of the Seifert surface (Lemma 3.5.14 [Gei]).

One can check that these two numbers are invariants of Legendrian knots in \mathbb{R}^3 by using the Legendrian Reidemeister moves. Let us see how to calculate these two invariants of an (oriented) Legendrian knot γ in \mathbb{R}^3 using the front projection. Recall that the *writhe* of a knot diagram is the sum (over the crossings in the diagram) of ± 1 at each crossing, where the sign is determined by handedness of the crossing (see Figure 2.5). We denote it by $w(\gamma)$.

Given an oriented knot, we define the upward cusps and the downward cusps as shown in Figure 2.6. The Thurston-Bennequin number and the rotation number of a Legendrian knot γ in front projection can be calculated as follows [Etn]:

$$tb(\gamma) = -\frac{1}{2}(\#\text{cusps}) + \#\text{positive crossings} - \#\text{negative crossings}.$$

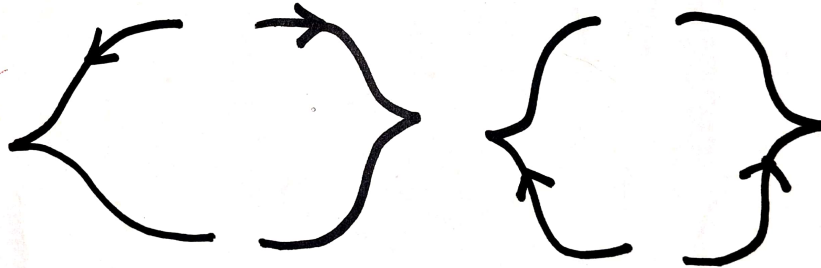


Figure 2.6: Downward and upward cusps.

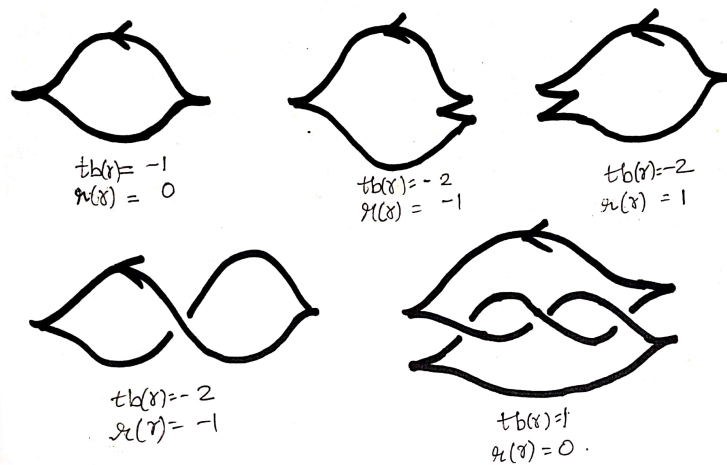


Figure 2.7: Calculation of Thurston-Bennequin number and rotation number [Hon].

$$r(\gamma) = \frac{1}{2} (\#\text{downward cusps} - \#\text{upward cusps}).$$

Figure 2.7 shows the Thurston-Bennequin number and rotation number of the unknot in four different Legendrian front projections and a trefoil knot. Note that if the number of crossings is zero then $|r(\gamma)| \leq tb(\gamma)$.

2.2 Legendrian surgery

One way to construct new 3-manifolds from old ones is by *Dehn surgery*. Let K be an oriented knot in S^3 with neighbourhood $N(K)$. Identify a right handed meridian μ

and a longitude λ on $\partial N(K)$, where λ lies in a Seifert surface for K . We can specify a framing on K by choosing a single nowhere-zero transverse vector field v to K . Given a null-homologous knot K , a Seifert surface provides the canonical framing λ_Σ given by the normal vector of the surface. We perform Dehn surgery on K with slope $\frac{a}{b}$ by constructing a 3-manifold

$$Y = (S^1 \times D^2) \cup_f \overline{S^3 \setminus N(K)}$$

where the gluing map $f : S^1 \times \partial D^2 \rightarrow \partial N(K)$ sends $\{*\} \times \partial D^2$ to the curve $a\mu + b\lambda$ [GoS].

We would like to know how Dehn surgery changes the contact structure. In the contact world, we have Legendrian knots. When we perform surgery on a Legendrian knot the natural framing to use is contact framing. Let's understand surgery on a contact manifold.

For a Legendrian knot γ , the contact framing λ_{tb} is given by oriented normal vectors to γ in ξ . Given a Legendrian knot in \mathbb{S}^3 , λ_{tb} corresponds to $tb(K)\mu + \lambda_\Sigma$ [Gei].

Let γ be a Legendrian knot in a 3-manifold M . A contact a/b surgery on γ is a topological $\frac{a}{b}$ surgery on γ with respect to the contact framing, and extending the contact structure on $M \setminus N(\gamma)$ across $S^1 \times D^2$ by a tight contact structure on $S^1 \times D^2$ [G]. We perform contact surgery on γ with slope $\frac{a}{b}$ by constructing a 3-manifold

$$Y = (S^1 \times D^2) \cup_f \overline{S^3 \setminus N(\gamma)}$$

where the gluing map $f : S^1 \times \partial D^2 \rightarrow \partial N(\gamma)$ sends $\{*\} \times \partial D^2$ to the curve $a\mu + b\lambda_{tb}$.

We have to check if such a surgery is well defined. For that we need the classification of tight contact structures on solid tori. We defer this classification to the next chapter but for continuity state the results here. There is no tight contact structure on a solid torus for $\frac{a}{b} = 0$. If $\frac{a}{b} = \frac{1}{n}$ there is a unique tight contact structure on the solid torus and therefore the surgery is well defined. For general $\frac{a}{b}$ there might not be a unique tight contact structure on the solid torus and hence contact surgery might not be well defined [G].

A *Legendrian surgery* on a Legendrian knot is a contact (-1) surgery along K . The reason we define Legendrian surgery specifically is that it preserves tightness [Wan]. For that we first need to know a special type of complex 2-manifolds called Stein manifolds.

A smooth, oriented, 4-manifold with boundary X^4 admits a *Stein structure* or is called a *Stein manifold* if and only if it has a handle decomposition satisfying all the conditions given in the following theorem.

Theorem 2.3 ([Eli4]). *A smooth, oriented, open 4-manifold X admits a Stein structure if and only if it is the interior of a (possibly infinite) handlebody such that the following hold:*

- (a) *Each handle has index ≤ 2 ,*
- (b) *Each 2-handle h_i is attached along a Legendrian curve γ_i in the contact structure induced on the boundary of the underlying 0- and 1-handles, and*
- (c) *The framing for attaching each h_i is obtained from the canonical framing on γ_i by adding a single left (negative) twist.*

A contact manifold M is called *holomorphically fillable* if it is the oriented boundary of a compact Stein surface. It is proved by Eliashberg and Gromov that holomorphically fillable structures are tight [Eli2]. Furthermore, there is the following theorem by Eliashberg.

Theorem 2.4 ([Eli2]). *If (M', ξ') is a contact manifold, obtained from a holomorphically fillable contact manifold (M, ξ) by Legendrian surgery, then (M', ξ') is holomorphically fillable.*

It is proved by Eliashberg [Eli1] that S^3 with the standard contact structure is holomorphically fillable. Using Theorem 2.4 we can construct tight contact structures by Legendrian surgery on knots in S^3 with the standard contact structure. The following theorem gives a necessary condition for two such tight contact structures to be isotopic.

Theorem 2.5 ([LM]). *Let X be a smooth 4-manifold with boundary. Suppose J_1 and J_2 are two Stein structures on X . Let $c(J)$ be the Chern class of the Stein structure J . If the induced contact structures on ∂X are isotopic, then $c(J_1) = c(J_2)$.*

Chapter 3

Convex surface theory

In this chapter, we study embedded surfaces in contact manifolds. Let M be a 3-manifold with contact structure ξ , which could be tight or overtwisted. Before we define convex surfaces, we need to understand how ξ traces a singular line field on an embedded surface Σ . The majority of this chapter is based on [Gir2], [Pat],[Hon1], [Hon2], [Siv], [Etn].

The *characteristic foliation* on Σ comes from integrating the line field induced by ξ . The line field is given at each point by $\Sigma_\xi(p) = \xi_p \cap T_p\Sigma$. The singular points are points $p \in \Sigma$ where $\xi_p = T_p\Sigma$. Each integral curve is called a leaf of the singular foliation. We denote this singular foliation by Σ_ξ .

One can orient the characteristic foliation. Assume Σ and ξ are both oriented. Then a singular point p is positive (resp. negative) if $T_p\Sigma$ and ξ_p have the same orientation (resp. opposite orientation). For a nonsingular point p of a leaf L , we choose the orientation to be given by a vector $v \in T_p(L)$ such that (v, n) is an oriented basis for $T_p\Sigma$, where $n \in T_p\Sigma$ is an oriented normal vector to ξ_p .

There are generically two types of isolated singularities: elliptic and hyperbolic [Hon]. Choose oriented coordinates (x, y) on Σ and let the singularity be at the origin. We write the contact structure as $\ker \alpha$ where $\alpha = dz + f dx + g dy$. Then $\Sigma_\xi = g \frac{\partial}{\partial x} - f \frac{\partial}{\partial y}$ is the vector field corresponding to the characteristic foliation near the origin. If the determinant of the matrix:

$$\begin{pmatrix} \frac{\partial g}{\partial x} & \frac{\partial g}{\partial y} \\ -\frac{\partial f}{\partial x} & -\frac{\partial f}{\partial y} \end{pmatrix}$$

is positive (resp. negative), then the singular point is elliptic (resp. hyperbolic). An example of a foliation with an elliptic singularity at the origin is given by the contact structure $\alpha = dz + x dy - y dx$, and an example of a foliation with a hyperbolic singularity

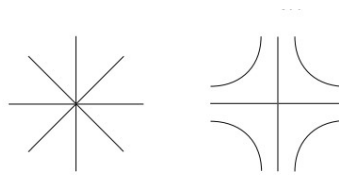


Figure 3.1: Elliptic and hyperbolic singularities [Hon].

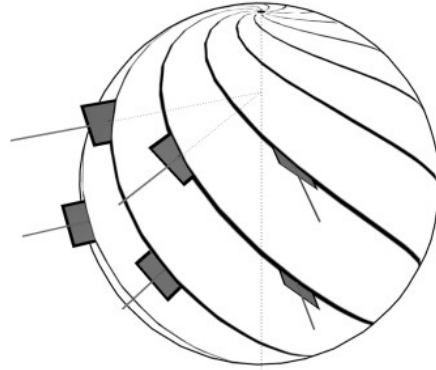


Figure 3.2: Characteristic foliation on unit sphere in \mathbb{R}^3 [Pat].

is given by the contact structure $\alpha = dz + xdy + ydx$. Figure 3.1 shows the leaves of characteristic foliations around elliptic and hyperbolic singularities. Now let us look at some examples and illustrations of characteristic foliations in different contact manifolds.

Consider a unit sphere centered at the origin in \mathbb{R}^3 with the contact structure given by $\ker(dz + r^2d\theta)$. We can see in [Pat] that this contact structure is contactomorphic to the standard contact structure on \mathbb{R}^3 . The characteristic foliation will have singularities at the intersection of the sphere and z -axis. All the leaves go from one singularity to another. Figure 3.2 shows some of the leaves of this characteristic foliation.

For our next example, consider T^3 with the contact structure given by $\ker(\cos(z)dx - \sin(z)dy)$. Figure 3.3 shows some planes of this contact structure. Here, opposite faces of the cube are glued to get T^3 . In this T^3 , consider a torus $x = \text{constant}$. We see two circles made entirely of singularities where $\sin(z) = 0$. One is at the top and bottom face of the cube while the other is in the middle. Figure 3.4 shows one such torus with the characteristic foliation on it. The arrows show the direction of the flow.

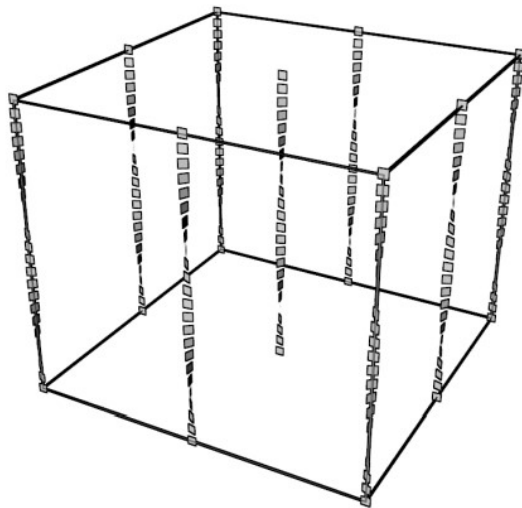


Figure 3.3: Contact structure on T^3 [Pat].

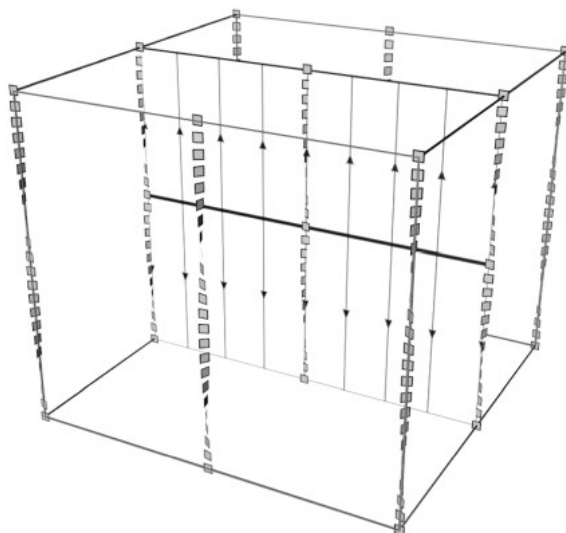


Figure 3.4: Characteristic foliation on $x = \text{constant}$ in T^3 [Pat].

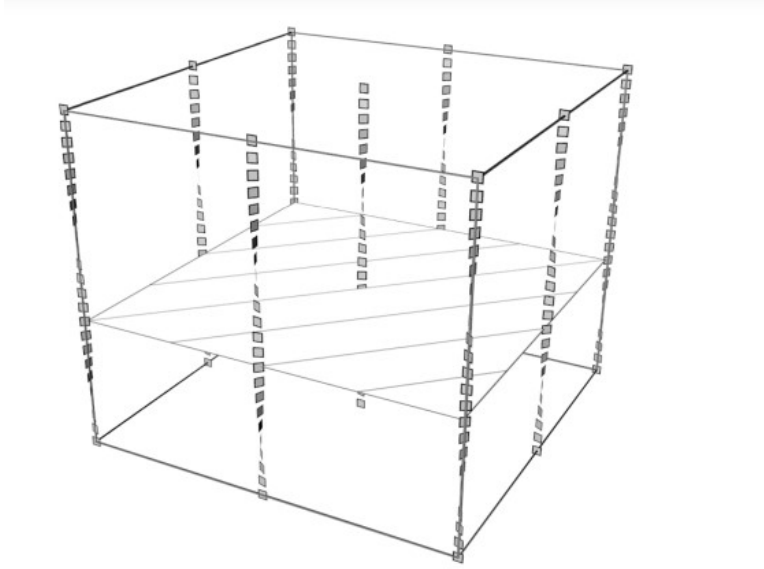


Figure 3.5: Characteristic foliation on $z = \text{constant}$ in T^3 [Pat].

Now let us look at a torus $z = \text{constant}$. On this torus, we get a characteristic foliation which has no singularities. Figure 3.5 shows some leaves of the characteristic foliation on a torus $z = \text{constant}$.

3.1 Dividing set

The theory and results in this section are due to Giroux [Gir1].

An embedded surface Σ in a contact 3-manifold $(M, \xi = \ker \alpha)$ is *convex* if there exists a vector field X on M which is transverse to Σ such that its flow preserves the contact structure. Such a vector field is called a *contact vector field* for ξ . The flow of the vector field X preserves the contact structure, which means that the Lie derivative of α is a real multiple of α , that is,

$$\mathcal{L}_X(\alpha) = \lambda\alpha.$$

This can be calculated using Cartan's magic formula:

$$\mathcal{L}_X(\alpha) = i_X(d\alpha) + d(i_X\alpha).$$

As an example of a convex surface, let us look at the unit sphere S^2 centered at the origin in (\mathbb{R}^3, ξ) where the contact structure is given by $\ker \alpha = \ker(dz + xdy - ydx)$. This contact structure is contactomorphic to the standard contact structure on \mathbb{R}^3 [Pat]. If

this sphere is convex, then there exists a contact vector field that is transverse to this sphere. Let us try with $X = x\partial x + y\partial y + z\partial z$. Using Cartan's magic formula we have,

$$\begin{aligned}
\mathcal{L}_X(\alpha) &= i_X(d\alpha) + d(i_X\alpha) \\
&= i_X(2dx \wedge dy) + d(\langle \alpha, x \rangle) \\
&= 2(i_X(dx) \wedge dy - dx \wedge (i_X(dy))) + d\langle dz + xdy - ydx, x\partial x + y\partial y + z\partial z \rangle \\
&= 2xdy - 2ydx + d(z + xy - yx) \\
&= 2xdy - 2ydx + dz.
\end{aligned}$$

This is not a contact vector field. The calculation before suggests trying with $X = x\partial x + y\partial y + 2z\partial z$. Then we get,

$$\begin{aligned}
\mathcal{L}_X(\alpha) &= 2xdy - 2ydx + 2dz \\
&= 2\alpha.
\end{aligned}$$

This X is a contact vector field. One can check that this X is transverse to S^2 . Hence, the unit sphere is convex in $(\mathbb{R}^3, \xi_{std})$.

The proposition from [Gir2] shows that convex surfaces are generic.

Proposition 3.1. *A closed, oriented embedded surface in a contact 3-manifold can be deformed by a C^∞ -small isotopy into a convex surface.*

If two characteristic foliations on a convex surface have the same leaves then we say they are equal. The proposition below tells us the importance of characteristic foliations in the context of contact structures.

Proposition 3.2 ([Gei]). *Let ξ_0 and ξ_1 be two contact structures on a 3-manifold M , which induce equal characteristic foliations on an oriented convex surface Σ . Then there is a neighbourhood of Σ on which ξ_0 and ξ_1 are isotopic.*

When we have a convex surface Σ in M , we define its *dividing set* Γ_Σ to be $\{x \in \Sigma \mid X(x) \in \xi_x\}$. We can think of the dividing set as those points where ξ is perpendicular to Σ , where perpendicular is measured with respect to X . We write $\#\Gamma_\Sigma$ for the number of connected components of Γ_Σ .

The following are significant properties of the dividing set which are proved in [Gir2]. The dividing set Γ_Σ is a multicurve, which is a properly embedded (smooth) 1-manifold, possibly disconnected and possibly with boundary. The isotopy class of Γ_Σ does not depend on the choice of our contact vector field X . The set Γ_Σ is nonempty. We can

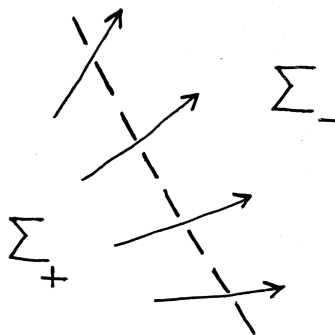


Figure 3.6: Characteristic foliation near the dividing set Γ_Σ [Pat].

divide the complement of Γ_Σ in Σ as $\Sigma_+ \sqcup \Sigma_-$, where Σ_+ (resp. Σ_-) is the set of points x where the normal orientation to Σ given by $X(x)$ agrees with (resp. is opposite to) the normal orientation to ξ_x . The term *sign configuration* on a convex surface with dividing curves means the induced sign in the complement of the dividing curves. Then as we across a dividing curve, we go from Σ_\pm to Σ_\mp . Figure 3.6 shows the characteristic foliation near a dividing curve. Notice that when we say dividing set we mean the dividing curves and the signs configuration on Σ .

Consider the convex torus of Figure 3.4. It has two dividing curves shown in dashed lines in Figure 3.7. In the next section we look at usefulness of dividing set especially when the convex surface is a torus.

3.1.1 Giroux's flexibility and Giroux's criterion

The usefulness of the dividing set comes from the following theorem by Giroux:

Theorem 3.3 (Giroux's flexibility theorem [Gir2]). *Consider a contact 3-manifold (M, ξ) and $\Sigma \subset M$ a convex surface with characteristic foliation Σ_ξ , contact vector field X and dividing set Γ_Σ . Let \mathcal{F} be another singular foliation on Σ which also has dividing set Γ_Σ . Then there is an isotopy ϕ_t , $t \in [0, 1]$, of Σ in (M, ξ) such that $\phi_0 = id$ and $\phi_t|_{\Gamma_\Sigma} = id$ for all t , $\phi_t(\Sigma) \pitchfork X$ for all t and $\phi_1(\Sigma)$ has characteristic foliation \mathcal{F} .*

The key idea here is that it is the dividing set and not the exact characteristic foliation which contains the essential contact topology information in a neighbourhood of Σ [Gir2].

We say that a convex surface Σ in a 3-manifold (M, ξ) has a tight neighbourhood if there exists a neighbourhood $N(\Sigma)$ such that $\xi|_{N(\Sigma)}$ is a tight contact structure on

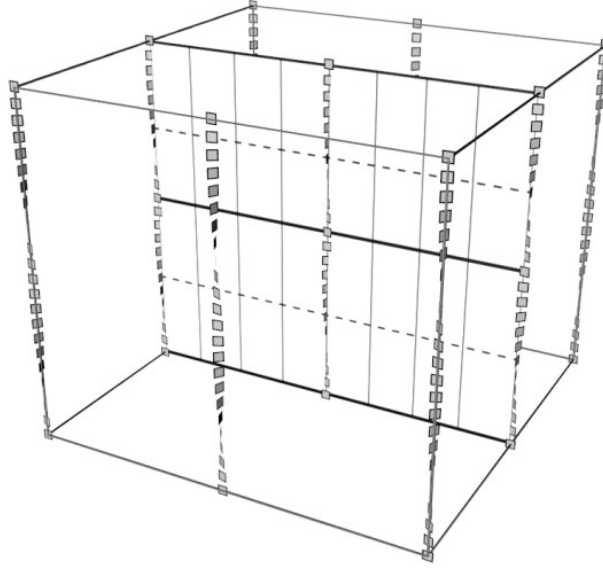


Figure 3.7: The dashed lines are the dividing set for the torus $x = \text{constant}$ [Pat].

$N(\Sigma)$. Now let us look at the criterion to determine when a convex surface has a tight neighbourhood.

Proposition 3.4. (*Giroux's criterion*) [Gir2] *A convex surface $\Sigma \neq S^2$ has a tight neighbourhood if and only if Γ_Σ has no homotopically trivial dividing curves. If $\Sigma = S^2$, then there is a tight neighbourhood if and only if $\#\Gamma_\Sigma = 1$.*

Let (M, ξ) be a 3-manifold with a tight contact structure. Say $\Sigma \cong S^2$ is a convex surface in M , then Γ_Σ is unique up to isotopy, consisting of one (homotopically trivial) circle. If $\Sigma \cong T^2$ is convex, then Γ_Σ consists of $2n$ parallel, homotopically essential curves. Once we fix a trivialisation $T^2 \cong \mathbb{R}^2/\mathbb{Z}^2$, Γ_{T^2} is determined by the number of dividing curves and the slope of those curves. For further details refer to [G].

One of the main ingredients we will need is the *convex torus in standard form* [Hon1]. Let T^2 be a convex torus in a tight contact manifold (M, ξ) . After some identification of T^2 to $\mathbb{R}^2/\mathbb{Z}^2$ the $2n$ dividing curves have slope $s \in \mathbb{Q} \cup \{\infty\}$. For a convex torus to be in the standard form we require a particular form of the characteristic foliation \mathcal{F} adapted to Γ_{T^2} . This characteristic foliation consists of parallel circles with a slope different from s hence they intersect Γ_{T^2} in points. Observe that singular points of such a foliation lie on curves parallel to Γ_{T^2} (necessarily alternating with Γ_{T^2}). We denote the set of these curves by \mathcal{L} . Each component of \mathcal{L} is called a *Legendrian divide*. A leaf of the characteristic foliation \mathcal{F} is called a *Legendrian ruling*. Let T^2 be a convex torus in standard form. We denote the slope of its dividing curves by s or $s(T^2)$ when we

want to specify the torus and we call it the slope of the torus. Say we have a 3-manifold M with convex torus as its boundary. By boundary slope we refer to the slope of the dividing curves on the boundary torus and denote it by $s(\partial M)$. If our manifold has multiple boundary tori, we index them by $\partial(M)_i$ and denote the slopes by $s(\partial(M)_i)$. The slope of the Legendrian ruling is denoted by r .

A consequence of Giroux's flexibility theorem can be formally stated as:

Corollary 3.5. (*Flexibility of Legendrian rulings*) *Let (T^2, ξ_{T^2}) be a torus in standard form. Via a continuous small perturbation near the Legendrian divides, we can modify the slope of the Legendrian rulings from r to any other $r' \neq s$ ($r = \infty$ included).*

3.1.2 Legendrian realisation

Given a curve or a collection of curves on a convex surface, how do we determine if they can be made to be Legendrian or not? We have a result which says that almost any curve can be realised as a Legendrian curve after perturbing a convex surface.

A union of properly embedded disjoint closed curves and arcs C on a convex surface Σ with Legendrian boundary are called *nonisolating* if

1. C is transverse to Γ_Σ and every arc of C begins and ends on Γ_Σ , and
2. every region of $\Sigma \setminus (\Gamma_\Sigma \cup C)$ has a boundary component which has some part of (or has some overlap with) Γ_Σ [Hon1].

Let X denote the contact vector field. An isotopy ϕ_s , $s \in [0, 1]$, for which $\phi_s(\Sigma) \pitchfork X$ for all s is called *admissible*.

Theorem 3.6. (*Legendrian realisation*) [[Hon1], Theorem 3.7] *Consider C , a nonisolating collection of disjoint properly embedded closed curves and arcs, on a convex surface Σ with Legendrian boundary. Then there exists an admissible isotopy ϕ_s , $s \in [0, 1]$ so that*

1. $\phi_0 = id$,
2. $\phi_s(\Sigma)$ are all convex,
3. $\phi_1(\Gamma_\Sigma) = \Gamma_{\phi_1(\Sigma)}$,
4. $\phi_1(C)$ is Legendrian.

Since ϕ_s is a contact isotopy, a nonisolating collection C can be realised by a Legendrian collection C' with the same number of geometric intersections with Γ_Σ . A corollary of this theorem is as follows:

Corollary 3.7. (*Kanda*) *A closed curve C on Σ which is transverse to Γ_Σ can be realised as a Legendrian curve (as in Theorem 3.6), if $C \cap \Gamma_\Sigma \neq \emptyset$.*

3.1.3 Twisting

In this section we will look at the twisting of our contact structure; first in a specific case, and then generalized. Our main reference is [Hon1].

Consider a tight contact structure ξ on $T^2 \times I$ with convex boundary. Identify the torus T^2 with $\mathbb{R}^2/\mathbb{Z}^2$ using an oriented identification. The slope $s(T^2)$ is defined by the property that each dividing curve is isotopic to a linear curve of slope $s(T^2)$ in T^2 identified with $\mathbb{R}^2/\mathbb{Z}^2$. Let $T_i = T^2 \times \{i\}$, s_i be the slope of the dividing curves on T_i and let $\alpha(s_i)$ be the angle between *ve* x -axis with the line of slope s_i in \mathbb{R}^2 . We say that slope s is between s_0 and s_1 if s is on the arc of the Farey tessellation as we go from s_0 to s_1 in clockwise direction. We say ξ is *minimally twisting* (in the I direction) if every convex torus parallel to the boundary has slope s between s_0 and s_1 . In particular, if ξ is minimally twisting and $s_0 = s_1$, then ξ is said to be *nonrotative* (in the I direction). We define I -twisting as $\beta_I = \alpha(s_0) - \alpha(s_1) = \sum_{k=1}^l (\alpha(s_{\frac{k-1}{l}}) - \alpha(s_{\frac{k}{l}}))$, where (i) $T_{\frac{i}{l}}$, $i = 0, 1, \dots, l$ are mutually disjoint convex tori parallel to the boundary, sequentially arranged from closest to farthest from T_0 , (ii) ξ is minimally twisting between $T_{\frac{k-1}{l}}$ and $T_{\frac{k}{l}}$ and (iii) $\alpha(s_{\frac{k}{l}}) \leq \alpha(s_{\frac{k-1}{l}}) \leq \alpha(s_{\frac{k}{l}}) + \pi$ [Hon1].

We will now look at another concept of twisting which is a generalisation of the Thurston-Bennequin number. The *twisting number* $t(\gamma, F)$ of a closed Legendrian curve γ with respect to a given framing F is the number of counterclockwise (right) 2π twists of the contact framing relative to F . If γ is null-homologous and F is the Seifert framing then the twisting number is equal to the Thurston-Bennequin number of γ and we denote it by $t(\gamma)$.

3.2 Bypasses

In this section, we learn how to change the dividing set on a convex surface. For this section, we mainly refer to [Hon].

Let $\Sigma \subset M$ be a convex surface (closed or compact with a Legendrian boundary). A *bypass* for Σ is an oriented embedded half-disk D with Legendrian boundary satisfying the following:

- (1) ∂D is the union of two arcs γ_1, γ_2 which intersect at their endpoints.
- (2) D intersects Σ transversely along γ_1 .
- (3) D (or D with opposite orientation) has the following singularities along ∂D :
 - (a) positive elliptic singularities at the endpoints of γ_1 (same as endpoints of γ_2),
 - (b) one negative elliptic singularity on the interior of γ_1 , and
 - (c) only positive singularities along γ_2 , alternating between elliptic and hyperbolic.

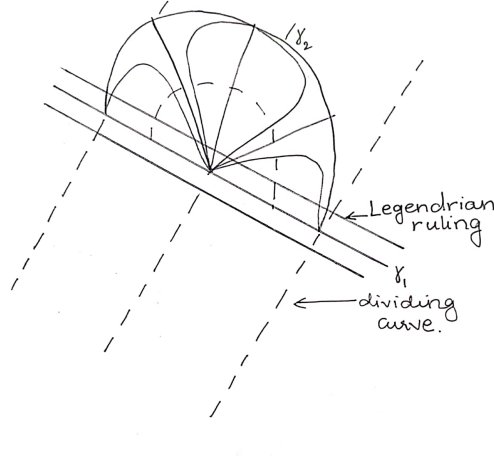


Figure 3.8: Bypass [GS].

(4) γ_1 intersects Γ_Σ exactly at three points, and these three points are the elliptic points of γ_1 .

We call the arc γ_2 a *bypass for Σ* or a *bypass for γ_1* . We define the *sign* of a bypass to be the sign of the elliptic point at the center of the half-disk. Figure 3.8 shows an illustration of a bypass disk attached on a convex surface. The disk is coming out of the page. The dashed lines are dividing curves on the convex surface.

Now let us see how attaching a bypass changes the dividing curves on a convex surface.

Lemma 3.8. (*Bypass attachment*)[Hon1] *Assume D is a bypass for a convex surface Σ in a contact 3-manifold (M, ξ) . Then there exists a neighbourhood of $\Sigma \cup D \subset M$ diffeomorphic to $\Sigma \times [0, 1]$, such that $\Sigma_i = \Sigma \times \{i\}$, $i = 0, 1$, are convex, $\Sigma \times [0, \epsilon]$ is I -invariant, $\Sigma = \Sigma \times \{\epsilon\}$, and Γ_{Σ_1} is obtained from Γ_{Σ_0} by performing the bypass attachment operation depicted in Figure 3.9 in a neighbourhood of the attaching Legendrian arc γ_1 .*

In Figure 3.9, the dotted lines are dividing curves and the solid line is a Legendrian arc of attachment of γ_1 .

Bypasses on tori

We specifically look at bypasses on tori because we need them for the classification of tight contact structures on $T^2 \times I$, which is one of the building blocks for constructing other 3-manifolds. We use [Hon1] as our main reference.

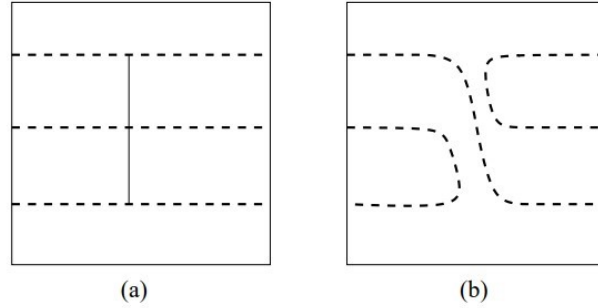


Figure 3.9: Dividing curves before and after bypass attachment [Hon1].

Let $\Sigma \subset M$ be a convex torus in standard form (refer to Section 3.1.1), identified with $\mathbb{R}^2/\mathbb{Z}^2$. We can assume that (with this identification) the Legendrian divides and rulings are linear. After acting via $SL(2, \mathbb{Z})$, we can assume that the slope of the dividing curves on Σ is $s = 0$ and that the ruling slope is a rational number r not equal to 0. Observe that we can normalize the Legendrian rulings via an element $\begin{pmatrix} 1 & m \\ 0 & 1 \end{pmatrix} \in SL(2, \mathbb{Z})$, $m \in \mathbb{Z}$, so that $-\infty < r \leq -1$.

Lemma 3.9. (*Layering*) *Assume a bypass D is attached to $\Sigma \cong T^2$ with slope $s(T^2) = 0$, along a Legendrian ruling curve of slope r with $-\infty < r \leq -1$. Then there exists a neighbourhood $T^2 \times I$ of $\Sigma \cup D \subset M$, with $\partial(T^2 \times I) \cong T_1 - T_0$, such that $\Gamma_{T_0} = \Gamma_\Sigma$, and Γ_{T_1} will be as follows, depending on whether $\#\Gamma_{T_0} = 2$ or $\#\Gamma_{T_0} > 2$:*

- (1) *If $\#\Gamma_{T_0} > 2$, then $s_1 = s_0 = 0$, and $\#\Gamma_{T_1} = \#\Gamma_{T_0} - 2$.*
- (2) *If $\#\Gamma_{T_0} = 2$, then $s_1 = -1$, and $\#\Gamma_{T_1} = 2$.*

Here s_i is the slope of the dividing curves on T_i .

The proof of Lemma 3.9 follows from the bypass attachment Lemma (3.8). Figure 3.10 shows the dividing curves before and after the attachment of a bypass in the two cases described in the Lemma.

Until now, we have assumed that the slope of the dividing curves is 0. Now let us see what happens when we have a rational slope. To do that, we interpret the bypass attachment Lemma in terms of the standard Farey tessellation of the hyperbolic unit disk $\mathbb{H}^2 = \{(x, y) \mid x^2 + y^2 \leq 1\}$. To get the Farey tessellation, start by labeling $(1, 0)$ as $0 = \frac{0}{1}$, and $(-1, 0)$ as $\infty = \frac{1}{0}$. We inductively label points on $S^1 = \partial\mathbb{H}^2$ as follows: For $y > 0$, start with $\infty \geq \frac{p}{q} \geq 0$ and $\infty \geq \frac{p'}{q'} \geq 0$ such that $(p, q), (p', q')$ form a \mathbb{Z} -basis of \mathbb{Z}^2 . Then, we label $\frac{p+p'}{q+q'}$ the point halfway between $\frac{p}{q}$ and $\frac{p'}{q'}$ along S^1 on

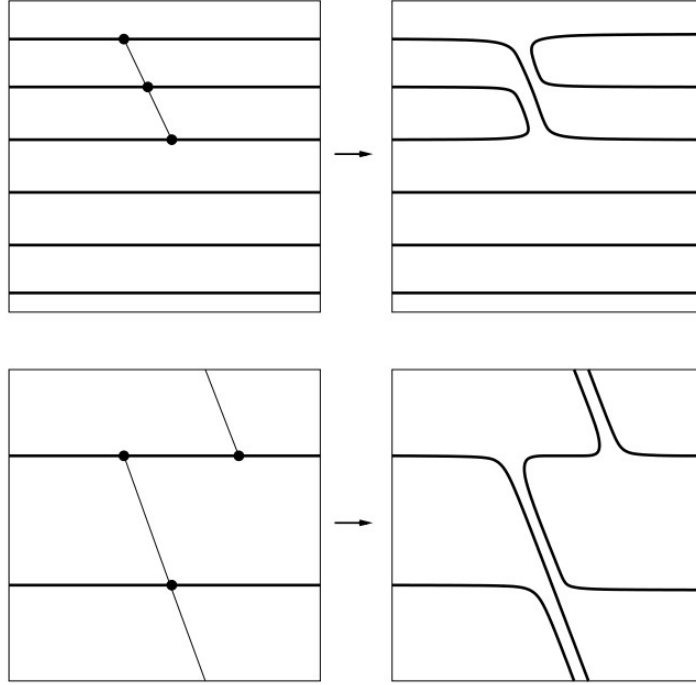


Figure 3.10: Bypass attachment on torus [Hon1].

the shorter arc (one for which $y > 0$ always). Two points $\frac{p}{q}$ and $\frac{p'}{q'}$ have an edge joining them in the Farey tessellation if $|pq' - qp'| = 1$. So we have a fraction $\frac{p}{q}$ assigned to each point $(x, y) \in S^1$ with $y > 0$. We assign the fraction $-\frac{p}{q}$ to the point $(x, -y) \in S^1$ and get edges in the same way as mentioned above. Figure 3.11 shows part of the Farey tessellation of a hyperbolic disk.

The next Lemma gives us the slope of the new dividing curves after we attach a bypass along a Legendrian ruling, when $\#\Gamma = 2$ and we know the slopes of the dividing curves and the Legendrian rulings before the bypass attachment.

Lemma 3.10. *Let $\Sigma \cong T^2$ be a convex surface with $\#\Gamma_{T^2} = 2$ and let the slope of the dividing curves on T^2 be s . If a bypass D is attached to Σ along a Legendrian ruling curve of slope $r \neq s$, then the resulting convex surface Σ' will have $\#\Gamma_{T^2} = 2$ and slope s' which is obtained as follows: Take the arc $[r, s] \subset \partial\mathbb{H}^2$ obtained by starting from r and moving counterclockwise until we hit s . On this arc, let s' be the point which is closest to r and has an edge in the Farey tessellation from s' to s .*

When we do a bypass attachment on a torus, we isotope the torus over the bypass

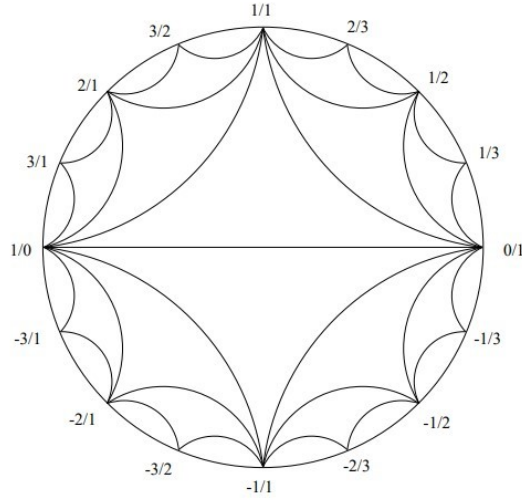


Figure 3.11: Farey tessellation of hyperbolic disk [Hon1].

disk and hence we say we have thickened the torus. Now let us look at an example to illustrate Lemma 3.9 point (2), using the recipe of Lemma 3.10. Start with a convex torus T^2 with $\#\Gamma_{T^2} = 2$ and $s(T^2) = 0$ and the slope of the Legendrian ruling $r = -2$. This is illustrated in the bottom left diagram in Figure 3.10. Figure 3.12 shows the arc from $r = -2$ to $s = 0$ in the counter clockwise direction. Then $s' = -1$ since it is the point which is the closest to $r = -2$ and has an edge in the Farey tessellation from s' to s . The bottom right diagram in Figure 3.10 shows the torus after attaching the bypass with the dividing curves with slope -1 .

Now let us see how can we find bypasses. The following two Lemmas [Hon1] tell us some ways in which bypasses can occur on a disk and on an annulus.

Lemma 3.11. *Let $\Sigma \cong D^2$ be a convex surface with Legendrian boundary inside a tight contact manifold, and $t(\partial\Sigma) = -n < 0$. Then every component of Γ_Σ is an arc which begins and ends on $\partial\Sigma$. There exists a bypass along $\partial\Sigma$ if $t(\partial\Sigma) < -1$.*

Lemma 3.12. *(Imbalance principle) Let $\Sigma \cong S^1 \times [0, 1]$ be convex with Legendrian boundary inside a tight contact manifold. If $t(S^1 \times \{0\}) < t(S^1 \times \{1\}) \leq 0$, then there exists a bypass along $S^1 \times \{0\}$.*

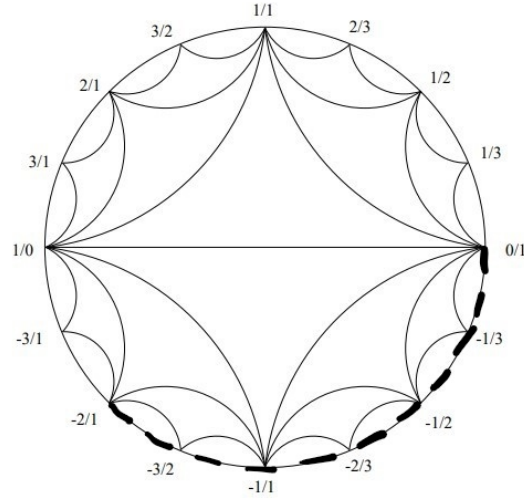


Figure 3.12: Arc in Farey tessellation from -2 to 0 [Hon1].

3.3 Classification of tight contact structures on basic blocks

The main strategy used when classifying tight contact structures on a given manifold M is to decompose M into simpler pieces, called basic blocks, by cutting along convex surfaces in M . These simpler pieces are the ones on which the classification of tight contact structures is known. In this section we study the classification on the basic blocks which we will use later for our classification theorem. Here, we present the classification of tight contact structures on B^3 , $T^2 \times I$ and $S^1 \times D^2$ up to isotopy. This section is based on [Hon1] and [GS].

Eliashberg [Eli3] gave the classification of tight contact structures on the 3-ball B^3 .

Theorem 3.13. *Two tight contact structures on the ball B^3 which coincide at ∂B^3 are isotopic relative to ∂B^3 .*

Now let us look at the classification of tight contact structures on $T^2 \times I$. We use characteristic foliations and bypass theory for the classification on $T^2 \times I$. Let us look at these before we state the classification results.

3.3.1 Flexibility of the characteristic foliations

Let M have a nonempty boundary, and \mathcal{F} be a characteristic foliation on ∂M which is adapted to a dividing set $\Gamma_{\partial M}$. Let $\text{Tight}(M, \mathcal{F})$ be the set of smooth tight contact structures ξ on M which induce the characteristic foliation \mathcal{F} on ∂M . The isotopy

3.3. CLASSIFICATION OF TIGHT CONTACT STRUCTURES ON BASIC BLOCKS 27

classes of tight contact structures on M with fixed boundary characteristic foliation \mathcal{F} are denoted by $\pi_0(\text{Tight}(M, \mathcal{F}))$. Giroux's flexibility theorem (Theorem 3.3) helps us prove the following:

Proposition 3.14. (*Flexibility lemma*) *Let M be a compact, oriented 3-manifold with nonempty boundary. Let \mathcal{F}_1 and \mathcal{F}_2 be two characteristic foliations on ∂M which are adapted to $\Gamma_{\partial M}$. There exists a bijection*

$$\phi_{12} : \pi_0(\text{Tight}(M, \mathcal{F}_1)) \rightarrow \pi_0(\text{Tight}(M, \mathcal{F}_2)) .$$

So we can write, $\text{Tight}(M, \Gamma)$ to stand for any of the $\text{Tight}(M, \mathcal{F})$, where \mathcal{F} is adapted to Γ .

3.3.2 Standard neighbourhood of Legendrian curve

Let $\gamma \subset M$ be a Legendrian curve with negative twisting number n with respect to a fixed framing. The *standard tubular neighbourhood* $N(\gamma)$ of γ is $S^1 \times D^2$ with coordinates $(z, (x, y))$ and contact 1-form $\alpha = \sin(2\pi n z)dx + \cos(2\pi n z)dy$. Here $\gamma = \{(z, (x, y)) | x = y = 0\}$. One can always perturb a neighbourhood of Legendrian knot to be contactomorphic to the standard tubular neighbourhood [Gei]. Fix the framing and identify $\partial N(\gamma) = \mathbb{R}^2/\mathbb{Z}^2$ by letting the meridian correspond to $(1, 0)^T$ and the longitude (from the framing) correspond to $(0, 1)^T$. Notice that $\partial N(\gamma)$ is a convex torus. With this identification, $s(\partial N(\gamma))$ is given by $-\frac{1}{n}$. Here is a result by Kanda [Kan], about the classification of tight contact structures in this neighbourhood, although phrased a bit differently.

Proposition 3.15. *Given a negative integer n , there exists a unique tight contact structure on $S^1 \times D^2$ with a fixed convex boundary with $\#\Gamma_{\partial(S^1 \times D^2)} = 2$ and slope $s(\partial(S^1 \times D^2)) = \frac{1}{n}$. Modulo modifying the characteristic foliation on the boundary using the flexibility Lemma, the tight contact structure is isotopic to the standard neighbourhood of a Legendrian curve with twisting number n .*

We will use the Lemma below a number of times for classifying tight contact structures.

Lemma 3.16. (*Twist number Lemma*) *Let (M, ξ) be a tight manifold. Consider a Legendrian curve γ with fixed framing Fr with $t(\gamma, Fr) = n \in \mathbb{Z}$, and a standard tubular neighbourhood, $N(\gamma)$ of γ with $s(\partial(N(\gamma))) = \frac{1}{n}$. If there exists a bypass D which is attached along a Legendrian ruling curve on $\partial(N(\gamma))$ of slope r , and $\frac{1}{r} \geq n + 1$, then there exists a Legendrian curve $N(\gamma)$, isotopic (but not Legendrian isotopic) to γ with larger twisting number.*

3.3.3 Basic slices

For this section the main reference is [Hon1]. Fix an identification $T^2 = \mathbb{R}^2/\mathbb{Z}^2$. Let $T^2 \times I = \mathbb{R}^2/\mathbb{Z}^2 \times [0, 1]$ with coordinates (x, y, z) , and $T_t = T^2 \times \{t\}$, $t \in [0, 1]$. Then $(T^2 \times I, \xi)$ is called a *basic slice* if

- (1) ξ is tight;
- (2) T_i are convex and $\#\Gamma_{T_i} = 2$, for $i = 0, 1$;
- (3) the minimal integral representatives of \mathbb{Z}^2 corresponding to s_i (for $i = 0, 1$) form a \mathbb{Z} -basis of \mathbb{Z}^2 ;
- (4) ξ is minimally twisting.

After a diffeomorphism of T^2 , we may assume that a basic slice has $s((T^2) \times \{1\}) = -1$ and $s((T^2) \times \{0\}) = 0$.

We denote the subset of minimally twisting tight contact structures in $\text{Tight}(T^2 \times I, \Gamma_{T_1} \cup \Gamma_{T_2})$ by $\text{Tight}^{\min}(T^2 \times I, \Gamma_{T_1} \cup \Gamma_{T_2})$.

Proposition 3.17. *Let $(T^2 \times I, \xi)$ be a basic slice with $\#\Gamma_{T_i} = 2$, $i = 0, 1$ and $s((T^2) \times \{1\}) = -1$ and $s((T^2) \times \{0\}) = 0$. Then $|\pi_0(\text{Tight}^{\min}(T^2 \times I, \Gamma_{T_1} \cup \Gamma_{T_2}))| = 2$.*

Hence, a basic slice can have two tight contact structures up to isotopy and fixed boundary characteristic foliation. We will call these positive and negative isotopy classes.

Here is a useful corollary of this result.

Corollary 3.18. *Let $(T^2 \times I, \xi)$ be a basic slice, with $s((T^2) \times \{1\}) = s_1$ and $s((T^2) \times \{0\}) = s_0$. Then for any slope s between s_1 and s_0 there exists a convex torus T parallel to $T^2 \times \{pt\}$ with slope $s(T) = s$.*

With this, one can prove the following proposition:

Proposition 3.19. *Let $(T^2 \times I, \xi)$ be tight with convex boundary and $s((T^2) \times \{1\}) = s_1$ and $s((T^2) \times \{0\}) = s_0$. Given any s between the s_0 and s_1 , there exists a convex torus parallel T to $T^2 \times \{pt\}$ with $s(T) = s$.*

3.3.4 Classification of tight contact structures on $T^2 \times I$

The main reference for this section is [Hon1]. Take $(T^2 \times I, \xi)$ such that ξ is tight, minimally twisting and rotative (refer 3.1.3). We will later look at the nonrotative case. We denote $s((T^2) \times \{1\})$ by s_1 and $s((T^2) \times \{0\})$ by s_0 . For convenience, adjust the slopes (using an action of $SL_2(\mathbb{Z})$) to be $s_0 = -1$ and $-\infty < s_1 < -1$. Write $s_1 = -\frac{p}{q}$ where $p \geq q > 0$ are integers and $(p, q) = 1$.

3.3. CLASSIFICATION OF TIGHT CONTACT STRUCTURES ON BASIC BLOCKS 29

Let $-\frac{p}{q}$ have the following unique continued fraction expansion:

$$-\frac{p}{q} = [a_0, \dots, a_k] = a_0 - \frac{1}{a_1 - \frac{1}{a_2 \cdots - \frac{1}{a_k}}},$$

with all $a_i < -1$ integers. We identify $-\frac{p}{q}$ with $[a_0, \dots, a_k]$.

Minimally twisting, rotative case

The classification of tight contact structures on $T^2 \times I$ is given in terms of the continued fraction expansion of the boundary slopes.

Proposition 3.20. *(Minimally twisting, rotative case) Let Γ_{T_i} , $i = 0, 1$, satisfy $\#\Gamma_{T_i} = 2$ and $s_0 = -1, s_1 = -\frac{p}{q}$, where $p > q > 0$. Then $|\pi_0(\text{Tight}^{\min}(T^2 \times I, \Gamma_{T_1} \cup \Gamma_{T_2}))| = |(a_0 + 1)(a_1 + 1) \cdots (a_{k-1} + 1)(a_k)|$.*

Minimally twisting, non-rotative case

Consider a contact structure ξ on $T^2 \times I$. Also assume that ξ is tight and minimally twisting; $\#\Gamma_{T_i} = 2, i = 0, 1$. For non rotative case we want that $s_0 = s_1$. Via an action of $SL_2(\mathbb{Z})$ we can have $s_0 = s_1 = -1$. The following proposition gives us the family of such tight contact structures on $T^2 \times I$ [Hon1].

Theorem 3.21. *(Minimally twisting, non rotative) Let Γ_{T_i} , $i=0,1$, satisfy $\#\Gamma_{T_i} = 2$ and $s_0 = s_1 = -1$. Then there exists a holonomy map $k : \pi_0(\text{Tight}^{\min}(T^2 \times I, \Gamma_{T_1} \cup \Gamma_{T_2})) \rightarrow \mathbb{Z}$, which is bijective.*

3.3.5 Giroux torsion

Say we have a contact manifold (M, ξ) . Say $T \subset M$ is a convex torus in standard form. For each $n \in \mathbb{Z}$, we say that (M, ξ) has n -torsion along T if there exists a contact embedding of $(T^2 \times I, \xi_n = \ker(\sin(2n\pi z)dx + \cos(2n\pi z)dy))$ into (M, ξ) , such that $T^2 \times \{t\}$ are isotopic to T . We say that (M, ξ) has n -Giroux torsion if there exists an embedded torus T along which (M, ξ) has n -torsion and there does not exist any embedded torus T' along which (M, ξ) has $(n + 1)$ -torsion [GH].

Chapter 4

Tight structures on Seifert manifolds

In this chapter we will be giving the proof of Theorem 1.1 and Theorem 1.2. First let us look at the construction of a large subfamily of Seifert fibred manifolds with four exceptional fibres. For details about Seifert fibred manifolds look at [Hat].

4.1 Seifert fibred 3-manifolds

A model Seifert fibring of $S^1 \times D^2$ is a decomposition of $S^1 \times D^2$ into disjoint circles called fibres. To construct it start with $I \times D^2$ and identify $0 \times D^2$ with $1 \times D^2$ using a $2\pi p/q$ rotation. Here $p/q \in \mathbb{Q}$ and $(p, q) = 1$. The segment that passes through the center of $I \times D^2$, that is $I \times \{0\}$, becomes one fibre. All the other fibres are made from q segments of $I \times \{x\}$.

A *Seifert fibring* of a 3-manifold M is a decomposition of M into disjoint circles, the fibres, such that each fibre has a neighbourhood fibre preserving diffeomorphic to a neighbourhood of a fibre in some model Seifert fibring of $S^1 \times D^2$. A Seifert manifold is one which possesses a Seifert fibring. In a Seifert manifold each fibre has a well defined multiplicity that is the number of times a small disk transverse to that fibre meets each nearby fibre. For example in the model Seifert fibring of $S^1 \times D^2$ with $2\pi p/q$ twist, the fibre $S^1 \times \{0\}$ has multiplicity q while all the other fibres have multiplicity 1. fibres of multiplicity 1 are called regular fibres and the others are called exceptional fibres. One can check that exceptional fibres are isolated and lie in the interior of M .

An explicit Seifert fibring can be constructed as follows: Start with B a compact, connected, orientable surface. Choose disjoint disks D_1, \dots, D_k in the interior of B . Let B' be B with the interiors of these disks deleted. Let $M' \rightarrow B'$ be the circle bundle with

M' orientable. Since B' is orientable M' is the product $B' \times S^1$. Let $s : B' \rightarrow M'$ be a section of $M' \rightarrow B'$. We choose a diffeomorphism of each component of $-\partial M'$ with $S^1 \times S^1$ by taking the section to $S^1 \times \{y\}$ and a fibre to $\{x\} \times S^1$. From M' we construct M by attaching k solid tori $V_i = D^2 \times S^1$ to the torus components of $-\partial M'$, taking a meridian circle ∂D^2 of $D^2 \times S^1$ to a circle of some finite slope $p_i/q_i \in \mathbb{Q}$ in $-\partial M'$. The attaching map $A_i : \partial V_i \rightarrow -\partial M'$ is given by $\begin{pmatrix} p_i & a_i \\ -q_i & b_i \end{pmatrix} \in SL(2, \mathbb{Z})$. Here a_i and b_i are chosen in such a way that $A_i \in SL(2, \mathbb{Z})$. Once the meridian disk is attached there is only one way to fill in a ball to complete the attachment of $D^2 \times S^1$. We denote Seifert fibred manifolds as $M(g; -q_1/p_1, \dots, -q_k/p_k)$, where g is the genus of the surface B . We define the *Euler number*, $e_0(M) = \sum_i \lfloor \frac{-q_i}{p_i} \rfloor$, where $\lfloor x \rfloor$ is the least integer not greater than x .

We first look at a specific example of a Seifert fibred 3-manifold with base surface S^2 and four exceptional fibres, $M(0; -1/2, -1/2, -1/2, -1/2)$. We start by constructing tight contact structures with zero Giroux torsion by Legendrian surgery to get a lower bound on the number of tight contact structures. These tight contact structures might be contact isotopic. To distinguish non-isotopic contact structures we use Lisca-Matić's result Theorem 2.5 which uses Chern numbers and Stein structures. To get the upper bound on the number of tight contact structures we use convex surface theory for which we decompose our manifold as shown in Figure 4.4. We start by maximising the twisting numbers of the exceptional fibres by attaching bypasses. Then we use Honda's classification of tight contact structures on each of the pieces in the decomposition of M [Hon2, Hon1]. We then glue these pieces together to construct M . It is possible to get an overtwisted contact structure when we glue two pieces with tight contact structures; we identify and discard such combinations. We look at the dividing curves on the convex surfaces we glue together to find overtwisted disks. Amongst the remaining combinations, we need to identify the isotopic ones from the others. We use relative Euler class [Hon1] to identify non-isotopic tight contact structures.

4.2 An example case

Theorem 4.1. *There are three tight contact structures with zero Giroux torsion on $M(0; -1/2, -1/2, -1/2, -1/2)$ up to contact isotopy. All three of them are Stein fillable. For each $n \in \mathbb{Z}^+$ there exists at least one tight contact structure with n -Giroux torsion on M . These tight contact structures are not weakly fillable.*

We start by constructing the manifold $M(0; -1/2, -1/2, -1/2, -1/2)$. We follow the method shown in Section 4.1. We start with the surface S^2 . Let B' be S^2 with the interior of four disks removed and M' be the orientable circle bundle over B' . The attaching maps

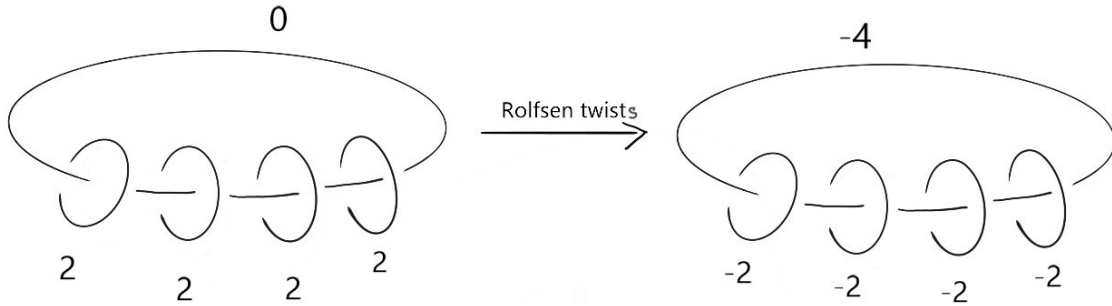


Figure 4.1: Surgery description of the Seifert manifold.

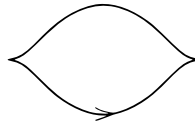


Figure 4.2: Legendrian realisation of unknot with Thurston-Bennequin number -1.

$A_i : \partial V_i \rightarrow -\partial M'$ are given by $\begin{pmatrix} 2 & -1 \\ 1 & 0 \end{pmatrix}$. The surgery representation of this manifold M is shown on the left hand side in Figure 4.1. We perform four (-1) Rolfsen twists to get the surgery diagram on the right in Figure 4.1. The Legendrian representation of an unknot with surgery coefficient -2 has Thurston-Bennequin number -1 and hence the rotation number is 0. This gives a unique Legendrian representation, for each of the four -2 framed unknots as shown in Figure 4.2. For the unknot with surgery coefficient -4 , the Legendrian realisation has Thurston-Bennequin number -3 and hence the rotation number can be $-2, 0$, or 2 . The corresponding Legendrian realisations are shown in Figure 4.3. Since the rotation numbers of these three Legendrian realisations are different, the Chern numbers of the corresponding Stein structures are different [LM]. Then, by Theorem 2.5, the three contact structures are non-isotopic. Since they are Stein fillable (using Lemma 2.4) they have zero Giroux torsion [Gay]. This tells us that there are at least three tight contact structures on M with zero Giroux torsion up to contact isotopy.

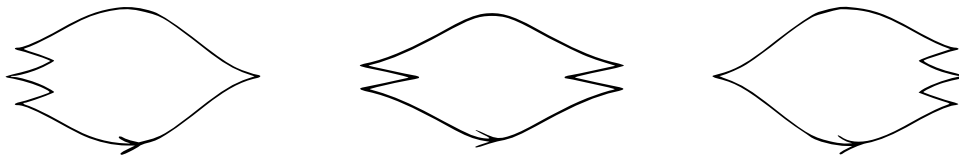


Figure 4.3: Legendrian realisations of the unknot with Thurston-Bennequin number -3.

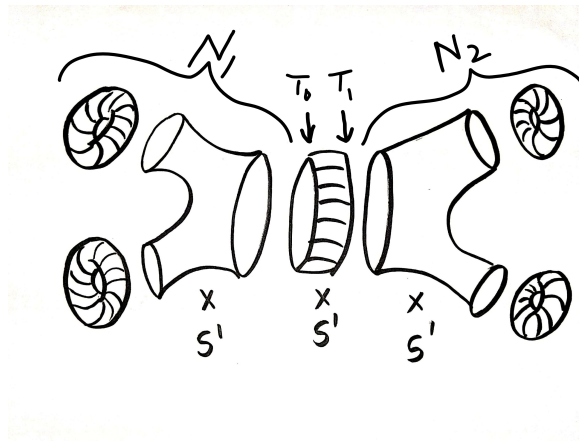


Figure 4.4: Decomposition of a Seifert fibred 3-manifold with four exceptional fibres.

4.2.1 Upper bound

A 3-manifold M is called *irreducible* if every 2-sphere $S^2 \subset M$ bounds a ball $B^3 \subset M$. A 2-sided surface $S \subset M$ without S^2 or D^2 components is called *incompressible* if for each disk $D \subset M$ with $D \cap S = \partial D$ there is a disk $D' \subset S$ with $\partial D' = \partial D$. An irreducible manifold M is called *atoroidal*, if every incompressible torus in M is ∂ -parallel; otherwise, the manifold is called *toroidal*. It is proved by Colin in [Col]:

Theorem 4.2. *Let M be an oriented, closed, connected, toroidal irreducible 3-manifold which contains an incompressible torus. Then M carries infinitely many isotopy classes of tight contact structures.*

The converse was later proved by Colin, Giroux and Honda in [CGH]:

Theorem 4.3. *Every closed, oriented, atoroidal 3-manifold carries a finite number of tight contact structures up to isotopy.*

The Seifert fibred 3-manifold with four exceptional fibres, $M = M(0; -1/2, -1/2, -1/2, -1/2)$ has infinitely many incompressible torus. We would like to count the tight contact structures on M with zero Giroux torsion. We have indicated one incompressible torus in Figure 4.4. Consider a $T^2 \times I$ neighbourhood of one of the incompressible tori. We cut along T_0 and T_1 to decompose our manifold in three pieces, one of which is $T^2 \times I$. The other two pieces are denoted by N_1 and N_2 . As shown in Figure 4.4 each N_i can be decomposed in $\{\text{pair of pants}\} \times S^1$ and two solid tori.

Let us start by looking at one of these pieces, say N_1 . We denote the $\{\text{pair of pants}\} \times S^1$ by $\Sigma \times S^1$ and the two solid tori by V_1, V_2 . There are three boundary components of $\Sigma \times S^1$, which we denote by $\partial(\Sigma \times S^1)_i$, where $\partial(\Sigma \times S^1)_i$ for $i = 1, 2$

corresponds to the torus ∂V_i for $i = 1, 2$ and $\partial(\Sigma \times S^1)_3$ is glued to the $T^2 \times I$. Note that $\partial(\Sigma \times S^1)_3$ is the same as ∂N_1 . We identify ∂V_i with $\mathbb{R}^2/\mathbb{Z}^2$ by choosing $(1, 0)^T$ as the meridional direction and $(0, 1)$ as longitudinal direction. We denote the two singular fibres by F_1 and F_2 and assume that these are simultaneously isotoped to Legendrian curves and further isotoped so that their twisting number is negative. Denote their twisting numbers by n_1 and n_2 . Let V_1 and V_2 be the standard neighbourhoods of F_1 and F_2 . The slope of the dividing curves (refer Section 3.1.1) on ∂V_i is $\frac{1}{n_i}$. Using the construction from Section 4.1, the two attaching maps $A_i : \partial V_i \rightarrow -\partial(\Sigma \times S^1)_i$ are given by $\begin{pmatrix} 2 & -1 \\ 1 & 0 \end{pmatrix}$ for $i = 1, 2$.

4.2.2 Maximising twisting numbers

We use the same methods to maximise the twisting number as illustrated in [EH]. For $i = 1, 2$ we have $A_i \cdot (n_i, 1)^T = (2n_i - 1, n_i)$. We denote the slope of the dividing curve on $-\partial(\Sigma \times S^1)_i$ by $s(\partial(\Sigma \times S^1)_i) = \frac{n_i}{2n_i - 1}$ (Refer to Section 3.3.2). Note that the slope of the dividing curves on $\partial(\Sigma \times S^1)$ is not ∞ . Using the flexibility of Legendrian ruling (Corollary 3.5) we may assume that the Legendrian ruling slope of $\partial(\Sigma \times S^1)_i$ for $i = 1, 2, 3$ is infinite.

Lemma 4.4. *We can increase the twisting numbers n_1 and n_2 up to 0.*

Proof. Consider an annulus $I \times S^1$ in M from $\partial(\Sigma \times S^1)_1$ to $\partial(\Sigma \times S^1)_2$ such that its boundary consists of Legendrian ruling curves on the tori. The boundary of this annulus intersects the dividing curves in $2(2n_i - 1)$ points respectively.

If $n_1 \neq n_2$ then, due to the imbalance principle (Lemma 3.12) there exists a bypass along a Legendrian ruling curve on either of the boundaries. Note that $A_i^{-1} = \begin{pmatrix} 0 & 1 \\ -1 & 2 \end{pmatrix}$ and hence the Legendrian ruling has slope 2 on ∂V_i . Using the twist number Lemma 3.16 we can attach a bypass and thicken V_i to V'_i increasing the twisting number as long as $n_i < 0$.

Say $n_1 = n_2$ and there is no bypass on the annulus $A = I \times S^1$ in M from $\partial(\Sigma \times S^1)_1$ to $\partial(\Sigma \times S^1)_2$. Then we cut $N_1 \setminus (V'_1 \cup V'_2)$ open along A . Note that the boundary of a neighbourhood of $A \cup V'_1 \cup V'_2$ is a piecewise smooth solid torus with four edges. We use the edge rounding Lemma (Lemma 3.11, [Hon1]) to smoothen these four edges. Since each rounding changes the slope by an amount of $-\frac{1}{4} \frac{1}{2n_1 - 1}$, the slope of the diving curves

on the boundary torus is

$$s(\partial(\Sigma \times S^1)_1) + s(\partial(\Sigma \times S^1)_2) - 4\left(\frac{1}{4} \frac{1}{2n_1 - 1}\right)$$

$$\frac{n_1}{2n_1 - 1} + \frac{n_1}{2n_1 - 1} - \frac{1}{2n_1 - 1} = 1.$$

This boundary torus is isotopic to ∂N_1 and identified with $\mathbb{R}^2/\mathbb{Z}^2$ in the same way as ∂N_1 . Hence the slope of the dividing curves on boundary torus $-\partial N_1$ is -1 .

Now take an annulus $I \times S^1$ from $\partial(\Sigma \times S^1)_1$ to ∂N_1 . For $n_1 < 0$ we have $2n_1 - 1 < -1$. Hence there exists a bypass by the imbalance principle 3.12 on V_1 until we increase n_1 up to 0. One can do a similar calculation for n_2 . Hence we can increase n_1 and n_2 until $n_1 = n_2 = 0$. □

4.2.3 Combining tight contact structures on basic blocks

We have $n_1 = n_2 = 0$. The slope of the dividing curves on $-\partial N_1$ is -1 , on $\partial(\Sigma \times S^1)_1$ is 0 and on $\partial(\Sigma \times S^1)_2$ is 0. Now we count the number of tight contact structures on $\{\text{pair of pants}\} \times S^1$ when the slope of the dividing curves on the three boundary tori are $0, 0, -1$. Again consider an annulus $I \times S^1$ from $\partial(\Sigma \times S^1)_1$ to $\partial(\Sigma \times S^1)_2$. Either there exists a bypass on both boundary components or not.

Case 1: If no bypass exists then we have the following conditions: According to the classification Lemma 5.1 of Honda [Hon2], $\Sigma \times S^1$ with such boundary slopes has a unique tight contact structure as shown in Figure 4.5 (Note that we are using the opposite sign convention to Honda's). Call it ξ_A . Using the A_i^{-1} the slope of the dividing curve on the boundary of V_i for $i = 1, 2$ is ∞ . By Proposition 3.15, there is exactly one tight contact structure on V_i for $i = 1, 2$. This gives a unique tight contact structure on N_1 .

Case 2: If there is a bypass then the cutting and rounding construction gives a torus of infinite slope after a bypass attachment. Then Honda's classification of tight contact structures on $\{\text{pair of pants}\} \times S^1$ (Lemma 5.1, [Hon2]) asserts that there exists a unique factorisation $\Sigma \times S^1 = \Sigma' \times S^1 \cup L_1 \cup L_2 \cup L_3$, where the L_i are $T^2 \times I$ with minimal twisting and all components of the boundary of $\Sigma' \times S^1$, denoted by $\partial(\Sigma' \times S^1)_i$, have dividing curves of ∞ slope. Figure 4.6 shows Σ and Σ' with their boundary slopes. Here we fix Σ to be $\Sigma \times \{0\}$ and Σ' to be $\Sigma' \times \{0\}$.

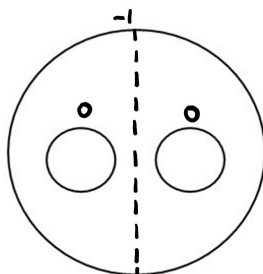


Figure 4.5: Dividing curve on Σ with contact structure ξ_A on $\Sigma \times S^1$.

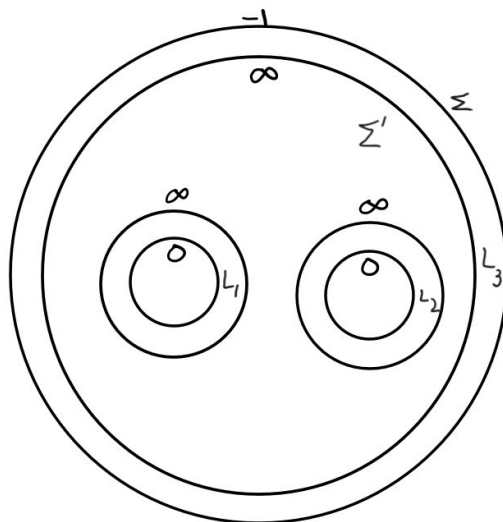


Figure 4.6: Σ and Σ' with their boundary slopes.

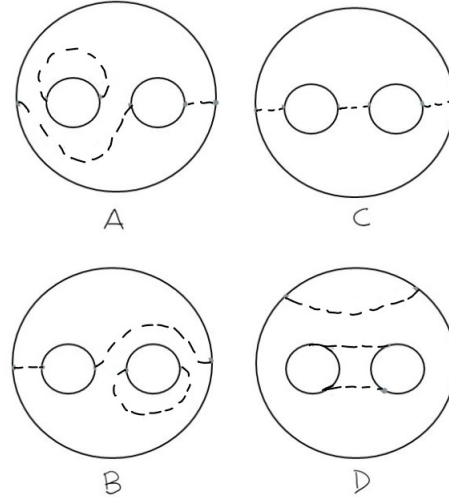


Figure 4.7: Possible dividing curves on pair of pants.

Let us start by looking at the tight contact structures on $\Sigma' \times S^1$ and then add in the L_i to get the tight contact structures on $\Sigma \times S^1$. Each boundary component of Σ' intersects the dividing set of the corresponding torus twice.

Lemma 4.5. *Each dividing curve on Σ' connects one boundary component to any other or one dividing curve goes from $\partial(\Sigma \times S^1)_3$ to itself and two dividing curves go from $\partial(\Sigma \times S^1)_1$ to $\partial(\Sigma \times S^1)_2$. These are shown in Figure 4.7 C,D.*

Proof. Assume there is a boundary-parallel dividing arc on boundary component one or on boundary component two as shown in Figure 4.7 A,B. Say the boundary parallel dividing arc is across $\partial(\Sigma \times S^1)_1$. This means there is a bypass along $\partial(\Sigma \times S^1)_1$. After attaching this bypass we can thicken $V_1 \cup L_1$ to get V'_1 . The slope on the boundary of V'_1 is 0 (using Lemma 3.10) in the basis of $\Sigma' \times S^1$. Hence we have a toric annulus L_1 with boundary slopes 0 and ∞ and an extension of this toric annulus is another toric annulus with boundary slopes ∞ and 0. Hence we have too much radial twisting in V'_1 and hence the contact structures on V'_1 is overtwisted. Similarly, we get an overtwisted contact structure if we had a boundary-parallel dividing arc on boundary component two. The possible dividing curves configurations without boundary-parallel dividing arcs on boundary component one or on boundary component two are of the form described in this Lemma. □

From the result in Lemma 4.5 we can divide our analysis in two cases, corresponding to Figure 4.7 C or D. These are two different dividing sets (refer to Section 3.1)

corresponding to different contact structures on $\Sigma \times S^1$. We will first count all the tight contact structures we get corresponding to Figure 4.7 C. We refer to this analysis as Case 2A. Then we do the same for Figure 4.7 D and refer to it by Case 2B.

Case 2A: Consider the set of dividing curves where each curve on Σ' connects one boundary component to the other as shown in Figure 4.7 C. The following Lemma is proved by Honda and Etnyre [EH]. I restate it for clarity.

Lemma 4.6. *The two dividing sets given by two different sign configurations (refer to 3.1) in Figure 4.7 C give a unique contact structure on $\Sigma' \times S^1$.*

Proof. We start by cutting $\Sigma' \times S^1$ along Σ' and then round the edges. We get a solid genus two handlebody. We can arrange the dividing curves on the boundary so that two meridional disks intersect the dividing set exactly twice. (This is shown in Figure 4.8.) Hence there is a unique dividing curve, separating the two intersection points, on these two disks. We cut along these two disks to get a 3-ball. There is a unique contact structure on this 3-ball with the given restriction to the boundary surface (Theorem 3.13). Since the dividing curves on the surface, we cut along are determined by our initial configuration of dividing curves, we get a unique contact structure on $\Sigma' \times S^1$. \square

Case 2B: Let us look at the case when one dividing curve goes from $\partial(\Sigma \times S^1)_3$ to itself and two dividing curves go from $\partial(\Sigma \times S^1)_1$ to $\partial(\Sigma \times S^1)_2$ as shown in Figure 4.7 D. This gives us at most two tight contact structures on $\Sigma \times S^1$ for Case 2B, one for each sign configuration.

We now look at the dividing curves on $\Sigma \times S^1 = \Sigma' \times S^1 \cup L_1 \cup L_2 \cup L_3$. Let $A_i = \Sigma \cap L_i$. For the contact structure on $\Sigma \times S^1$ to be tight the dividing set of A_3 will have two arcs connecting the boundary components. There are two possible configurations depending on the sign of the basic slice L_3 . The dividing set of A_1 and A_2 consists of a boundary parallel arc on the the boundary component with dividing curves of infinite slope. There are two possible configurations depending on the sign of the respective basic slice. This is shown in Figure 4.12. Again dotted lines represent the dividing curves. Now let us look at the dividing curves on $\Sigma \times S^1$ separately for case 2A and case 2B as we did before.

Case 2A: We fix one sign configuration for the contact structure on $\Sigma' \times S^1$ as shown in Figure 4.9. This fixes the sign configuration of the contact structure on L_3 . In our case it is positive. We write (\pm, \pm, \pm) to denote that the signs of the

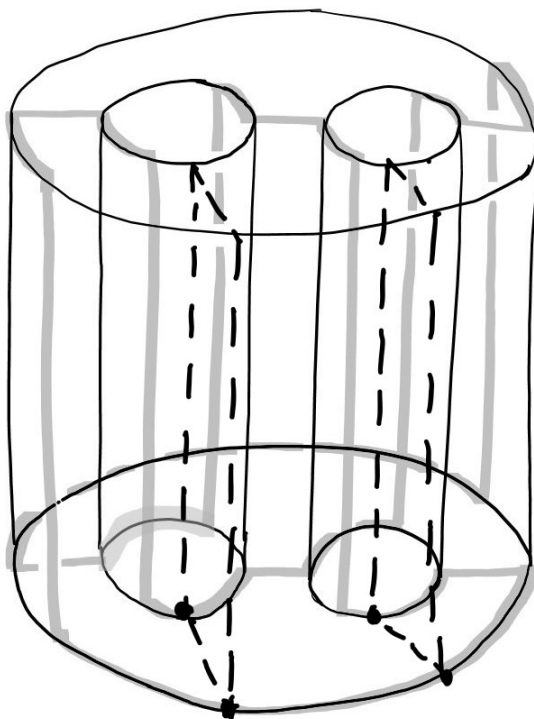


Figure 4.8: Dividing curves on boundary of $\Sigma' \times I$.

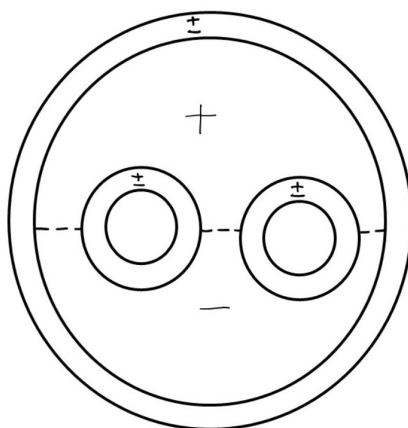


Figure 4.9: Possible dividing set on Σ .

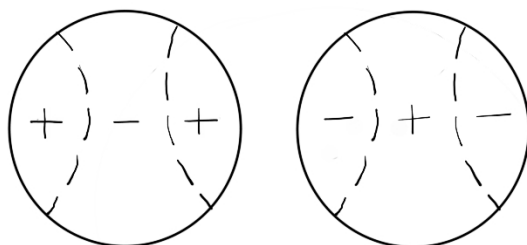


Figure 4.10: Two possibilities of dividing curves on \mathbb{D}^2 with $t(\partial\mathbb{D}) = 2$ [Hon1].

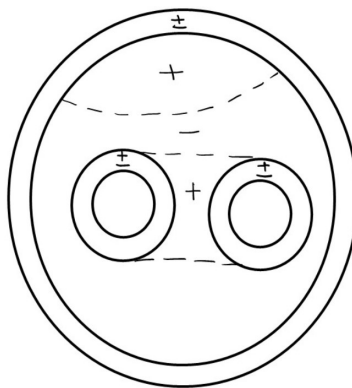


Figure 4.11: Possible dividing set on Σ .

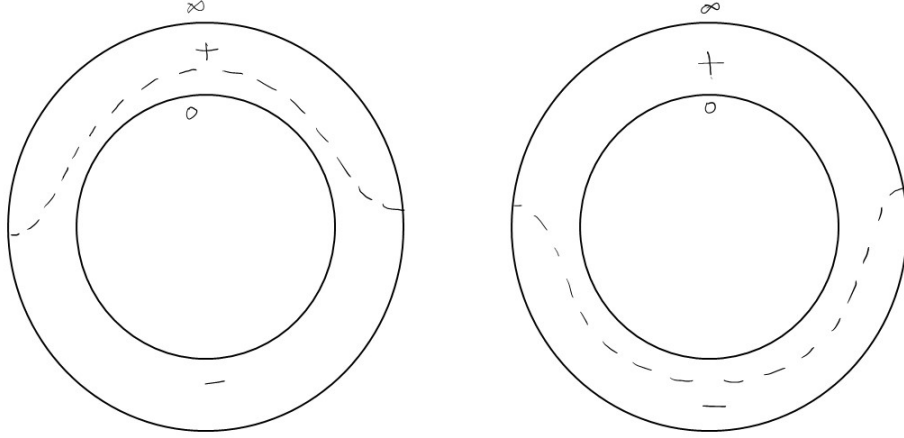


Figure 4.12: Positive (left) and Negative (right) sign configuration of dividing sets on A_2 and A_1 .

basic slices, L_i for $i = 1, 2, 3$ are positive/negative. Now we have a choice of sign for the contact structure on L_1 and L_2 . This gives us four total configurations, given by: $(+, +, +)$, $(-, -, +)$, $(-, +, +)$, $(+, -, +)$. It is proved in [Hon2] (Lemma 5.1, 9th paragraph in the proof) that if all three basic slices have the same sign then we get an overtwisted disk. Hence $(+, +, +)$ corresponds to an overtwisted contact structure on $\Sigma' \times S^1$.

We can have a contact structure with $(-, -, +)$ configuration. This corresponds to one tight contact structure on $\Sigma \times S^1$ with the slopes of the dividing curve on the boundary torus $0, 0, -1$. The dividing set is shown in Figure 4.13. The tight contact structure on $\Sigma \times S^1$ corresponding to this dividing set on Σ will be denoted by ξ_B . If we had started our case 2A with the opposite signed configuration, then we would have the dividing set as shown in Figure 4.14 on Σ . This corresponds to a different tight contact structure on $\Sigma \times S^1$. Let us call it $\xi_{B'}$.

Similarly we can have $(-, +, +)$ and $(+, -, +)$ configuration. The dividing sets corresponding to these signed configurations are shown in Figure 4.15. Each of these corresponds to one tight contact structure on $\Sigma \times S^1$. We denote them by ξ_C and ξ_D . If we had started our case 2A with the opposite signed configuration, then we would have the dividing sets shown in Figure 4.16 on Σ . These correspond to a different tight contact

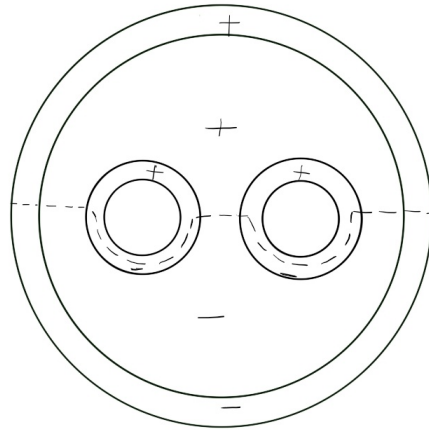


Figure 4.13: Dividing set of ξ_B on Σ .

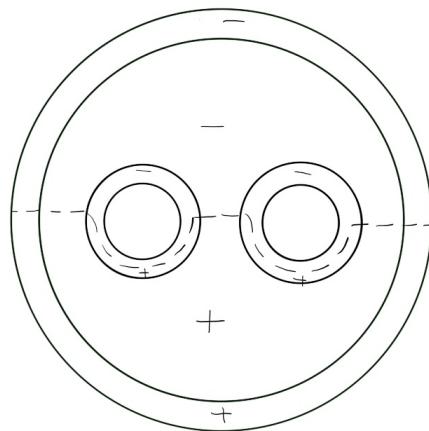


Figure 4.14: Dividing set of $\xi_{B'}$ on Σ .

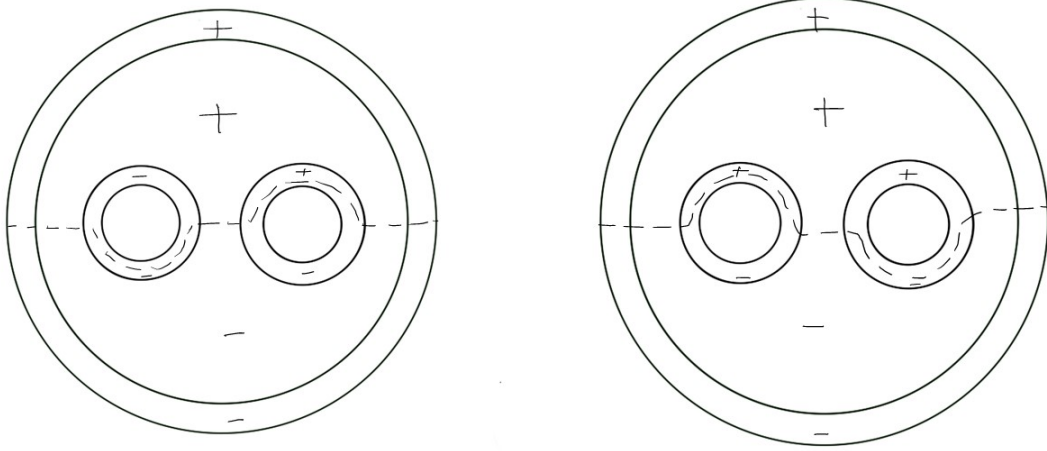


Figure 4.15: Dividing set of ξ_C and ξ_D on Σ .

structures on $\Sigma \times S^1$. Let us call them $\xi_{C'}$ and $\xi_{D'}$.

Case 2B: We have fixed one sign configuration for $\Sigma' \times S^1$ as shown in Figure 4.11. This fixes the sign configuration of L_3 . Now we have a choice for sign on L_1 and L_2 . This gives us four total configurations shown in Figure 4.17. The case where both the L_1 and L_2 have positive signs yields overtwisted contact structure. We can see the dividing curves by dotted lines in Figure 4.17 A. The boundary of the overtwisted disk is outside the disk bound by these dividing curves. Now consider the case when L_1 and L_2 have mixed signs. Then we get a bypass on the L_i with a negative sign as shown in Figure 4.17 B, C. Say the bypass is on L_1 . We can attach this bypass and thicken our solid torus to get a solid torus with boundary slope 0. Hence we have a toric annulus L_1 with boundary slopes 0 and ∞ and an extension of this toric annulus is another toric annulus with boundary slopes ∞ and 0. Hence we have too much radial twisting in V'_1 and hence the contact structures on V'_1 is overtwisted. Similarly, we get an overtwisted contact structure if we had a boundary-parallel dividing arc on boundary component two. Hence we are left with the case where both L_1 and L_2 have negative signs as shown in Figure 4.17 D. This contact structure on $\Sigma \times S^1$ is denoted by ξ_E . We would get the opposite signed configuration if we had started case 2B with the other sign configuration. This will be denoted ξ'_E and it is shown in Figure 4.18.

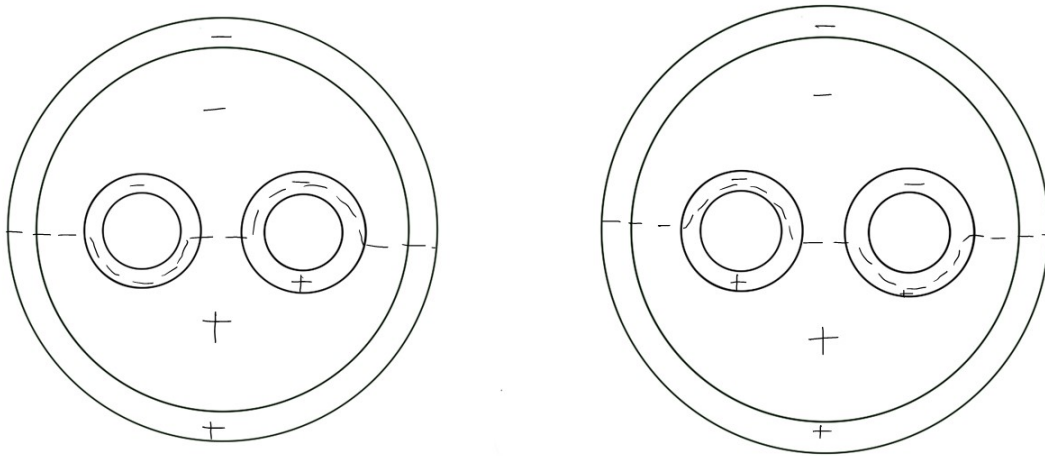


Figure 4.16: Dividing set of $\xi_{C'}$ and $\xi_{D'}$ on Σ .

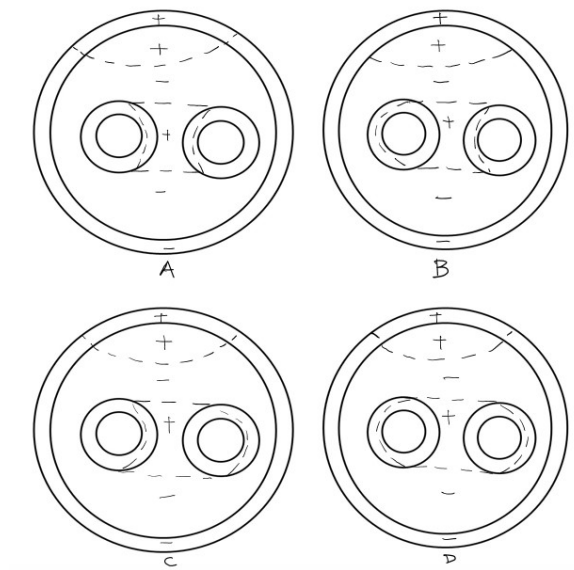
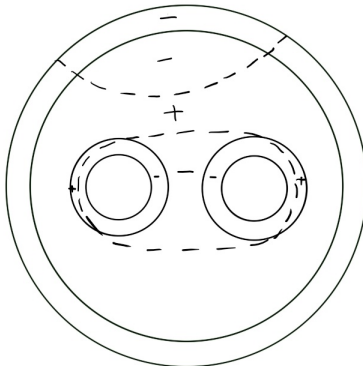


Figure 4.17: Four possible configurations of dividing curves on Σ .

Figure 4.18: Dividing set of $\xi_{E'}$ on Σ .

We have nine tight contact structures on $\Sigma \times S^1$ denoted by $\xi_A, \xi_B, \xi_{B'}, \xi_C, \xi_{C'}, \xi_D, \xi_{D'}, \xi_E, \xi_{E'}$. There is a unique tight contact structure on each V_i . Let us glue the two $\Sigma \times S^1$ along the toric annulus (refer section 4.2.1). When we are gluing the two $\Sigma \times S^1$ we are gluing using an orientation reversing diffeomorphism so we have to glue them using $T^2 \times I$ with boundary slopes -1 and $+1$. After gluing, we get $\{\text{sphere with four holes}\} \times S^1$, namely $\{\text{shirt}\} \times S^1$, which we call Y . Let us look at all possible tight contact structures on Y with zero Giroux torsion. Figure 4.19 shows all possible dividing curve configurations on the sphere with four holes which give potentially tight contact structures with zero Giroux torsion after gluing the two pairs of pants. The tight contact structure on Y we get by gluing two pairs of pants with ξ_E and $\xi_{E'}$ is shown in Figure 4.20. This contact structure has non-zero Giroux torsion (Section 3.3.5). All other combinations of gluing two pairs of pants give us an obvious overtwisted disk in Y .

When we glue the four solid tori to Y with contact structure as determined by the dividing curves in pictures 5,6,7 and 8 of Figure 4.19 we get overtwisted contact structures on $M(0; -1/2, -1/2, -1/2, -1/2)$. Indeed in all of these cases, there is a boundary parallel dividing curve, say γ_1 , on the shirt. There is a boundary parallel torus, say T_1 containing γ_1 . We denote this boundary torus as T_0 and the dividing curve on it as γ_0 . Consider the $T^2 \times [0, 1]$ from T_0 to T_1 . The dividing curves γ_0 and γ_1 have slope zero, hence we have a boundary parallel torus corresponding to every slope in this $T^2 \times I$ (Prop. 3.19). So in particular we have a torus with slope $\frac{1}{2}$. Using A_i^{-1} this

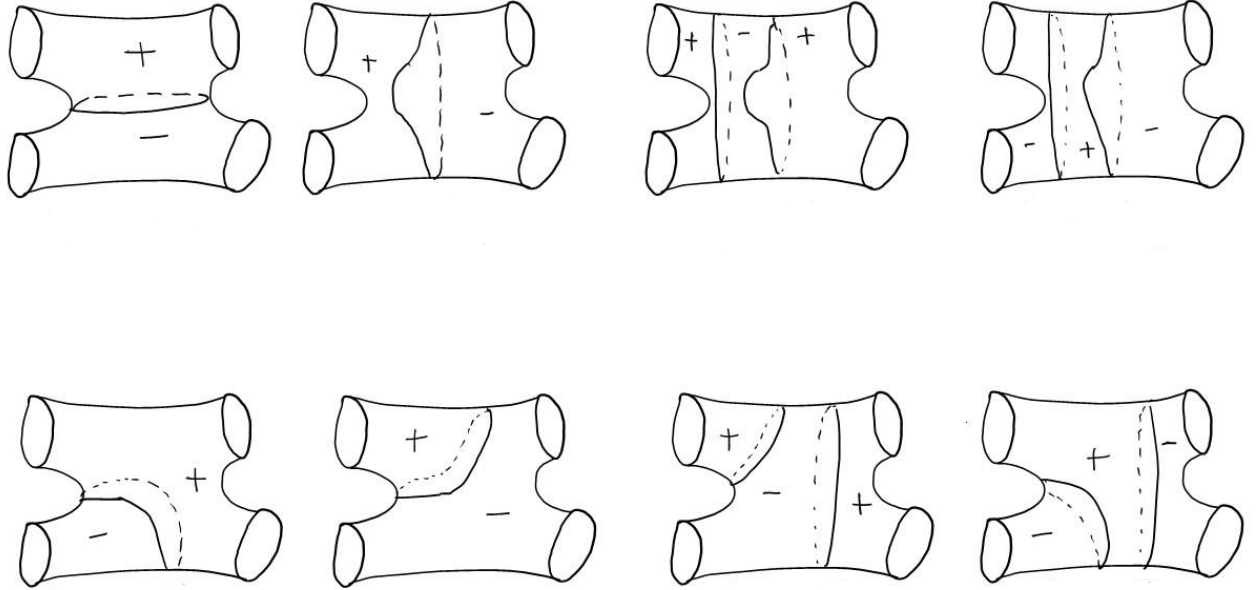


Figure 4.19: Dividing curve configurations on the sphere with four holes representing all possible tight contact structures on Y .

corresponds to slope zero in the basis of the glued in solid torus. Hence this dividing curve bounds a meridional disk in the solid torus which is our overtwisted disk.

We use the relative Euler class (see Section 4.2 in [Hon1]) to show that pictures 3 and 4 (as shown in Figure 4.19) yield non-isotopic tight contact structures on Y . We denote the i th tight contact structure in Figure 4.19 as ξ_i . We have that the relative Euler class $e(\xi_3) = -2$ whereas $e(\xi_4) = 2$. Diagrams 1 and 2 (as shown in Figure 4.19) can be shown to be equivalent by section changes similarly to those discussed in Section 4.3. The relative Euler class is $e(\xi_1) = 0$. So we get at most three potentially tight contact structures on $\{\text{shirt}\} \times S^1$.

Since the upper bound and lower bound (which we computed in Section 4.2) both are three, we get that $|\pi_0(\text{Tight}^{\min}(M))| = 3$. All of these are Stein fillable, since we get these three contact structures on M by doing a -1 Legendrian surgery on Legendrian link in (S^3, ξ_{std}) .

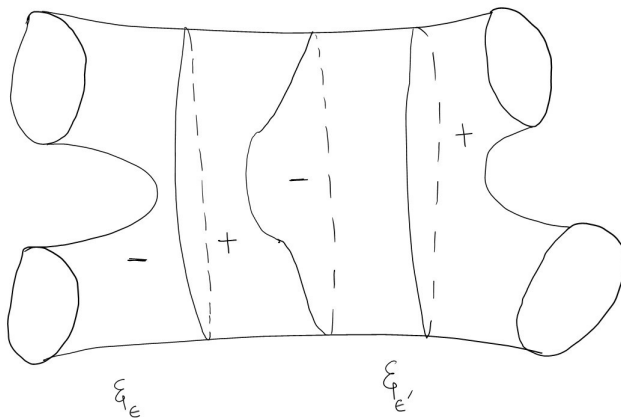


Figure 4.20: Dividing curve configuration on the sphere with four holes.

Since M is toroidal there are \mathbb{Z} many non-isotopic tight contact structures on M corresponding to integral Giroux torsion. It is proved by Gay in [Gay] that tight contact structures that are strongly symplectically fillable have no Giroux torsion. Also, it is proved in [Gei] that a weakly fillable tight contact structure on a rational homology sphere is a strongly fillable contact structure. The Seifert fibred manifold M is a rational homology sphere. Hence the tight contact structures on M with non-zero Giroux torsion are not weakly fillable.

4.3 General case

Consider the manifold $M = M(0; -q_1/p_1, -q_2/p_2, -q_3/p_3, -q_4/p_4)$ where $e_0 \leq -4$ (here Euler number, $e_0(M) = \lfloor \frac{-q_1}{p_1} \rfloor + \lfloor \frac{-q_2}{p_2} \rfloor + \lfloor \frac{-q_3}{p_3} \rfloor + \lfloor \frac{-q_4}{p_4} \rfloor$, where $\lfloor x \rfloor$ is the greatest integer not greater than x) and $p_i, q_i \in \mathbb{Z}$ with $p_i \geq 2$, $q_i \geq 1$ and $\gcd(p_i, q_i) = 1$, $\frac{-q_i}{p_i} = [a_0^i, a_1^i, \dots, a_{m_i}^i]$, where all a_j^i 's are integers, $a_0^i = \lfloor \frac{-q_i}{p_i} \rfloor \leq -1$, and $a_j^i \leq -2$ for $j \geq 1$. We define $p_j^i = -a_j^i p_{j-1}^i - p_{j-2}^i$ for $j = 0, 1, \dots, m_i$ and $p_{-2}^i = -1$ and $p_{-1}^i = 0$. Similarly we define $q_j^i = -a_j^i q_{j-1}^i - q_{j-2}^i$ for $j = 0, 1, \dots, m_i$ and $q_{-2}^i = -1$ and $q_{-1}^i = 0$. The previous example (Section 4.2) we have considered has $e_0(M) = -4$ and $\frac{-q_i}{p_i} = \frac{-1}{2}$. Once we have calculated the tight contact structures on this example case, it is computationally easy to generalise to the case of all manifolds M with $e_0(M) \leq -4$.

Theorem 4.7. *On M there are exactly $|(e_0(M) + 1) \prod_{i=1}^4 \prod_{j=1}^{m_i} (a_j^i + 1)|$ tight contact structures with zero Giroux torsion up to contact isotopy. All of these can be constructed by Legendrian -1 surgery and hence are Stein fillable. For each $n \in \mathbb{Z}^+$ there exists at least one tight contact structure with n -Giroux torsion on M . These tight contact structures are not weakly fillable.*

To prove this theorem we follow similar methods as we used for our example case

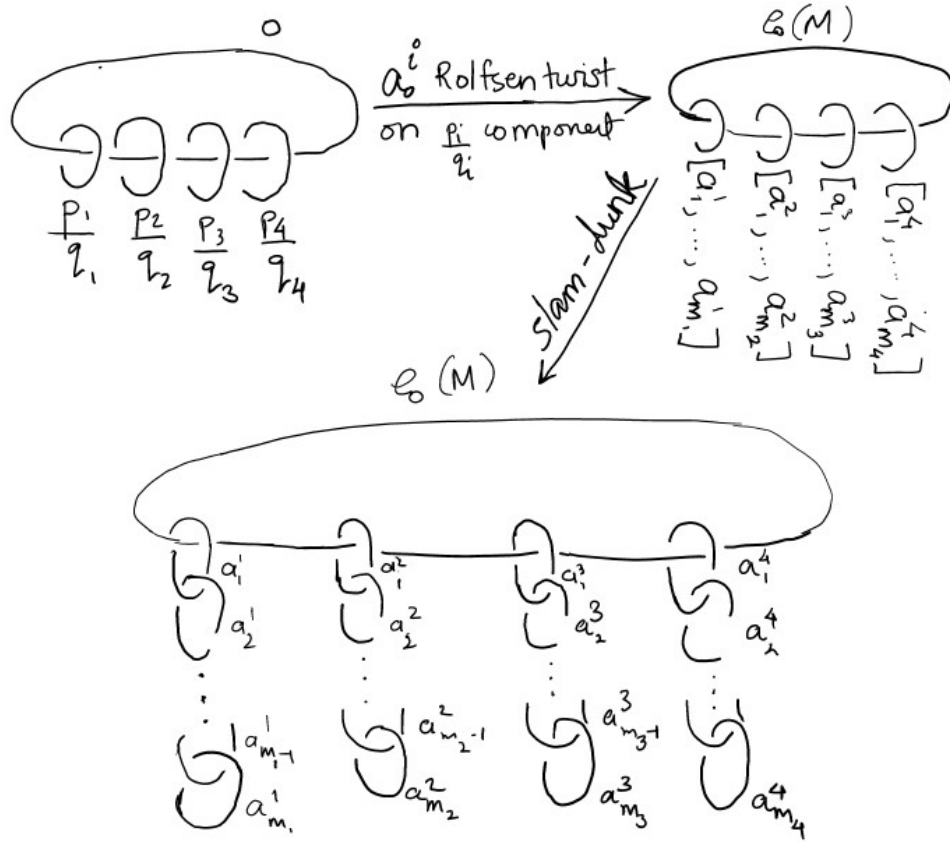


Figure 4.21: Surgery diagram representations of the manifold $M(0; -q_1/p_1, -q_2/p_2, -q_3/p_3, -q_4/p_4)$.

(see Section 4.2). We need an additional section change operation to show that some of the potential tight contact structures are isotopic.

The surgery diagram for the construction of $M = M(0; -q_1/p_1, -q_2/p_2, -q_3/p_3, -q_4/p_4)$ is shown in Figure 4.21 on top left. We perform Rolfsen twists to get the surgery diagram on the top right. We do a slam dunk operation to obtain the diagram at the bottom. One can refer to [GoS] for both these operations. The number of Legendrian realisations for each of the unknots is $(a_j^i + 1)$ or $(e_0(M) + 1)$ based on their Thurston-Bennequin and rotation numbers. Then by Theorem 2.5 there are at least $|(e_0(M) + 1) \prod_{i=1}^4 \prod_{j=1}^{m_i} (a_j^i + 1)|$ tight contact structures with zero Giroux torsion on M up to contact isotopy. This gives a lower bound on the number of tight contact structures on M .

Upper Bound

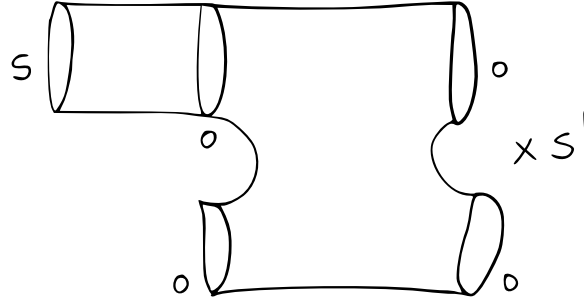
We start with the decomposition of the Seifert fibred manifold as stated previously in the example case. The manifold $M = M(0; -q_1/p_1, -q_2/p_2, -q_3/p_3, -q_4/p_4)$ has incompressible tori. We are going to start by counting tight contact structures with zero Giroux torsion on M .

Using the same construction and notations from the example case as in Figure 4.4 we have that the two attaching maps $A_i : \partial V_i \rightarrow -\partial(\Sigma \times S^1)_i$ are given by $\begin{pmatrix} p_i & u_i \\ q_i & v_i \end{pmatrix} \in SL_2(\mathbb{Z})$ for $i = 1, 2$ where $u_i = p_{m_i-1}^i$ and $v_i = q_{m_i-1}^i$. Using the flexibility of Legendrian ruling (Corollary 3.5) we assume that the ruling slope of $\partial(\Sigma \times S^1)_i$ for $i = 1, 2, 3$ is infinite. Assume that the fibres F_i are simultaneously isotoped to Legendrian curves such that their twisting numbers are particularly negative. For $i = 1, 2$ we have $A_i \cdot (n_i, 1)^T = (n_i p_i + u_i, n_i q_i + v_i)$. We denote the slope of the dividing curve on $-\partial(\Sigma \times S^1)_i$ by $s_i = \frac{n_i q_i + v_i}{n_i p_i + u_i} = \frac{q_i}{p_i} + \frac{1}{p_i(n_i p_i + u_i)}$.

Note that the manifolds, $M(0; -q_1/p_1, \dots, -q_4/p_4)$, we are working with are L-spaces (see Theorem 1.1 [LS]). We look at Seifert fibred manifold $M' = (0; -q_1/p_1, \dots, -q_3/p_3)$ which is an L-space with $e_0 \leq -2$. Any tight contact structures on M' has a Legendrian curve with twisting number -1 in the $\{\text{pair of pants}\} \times S^1$ (Using corollary 5.2 from [G]). We call this curve L and its neighbourhood V . We can construct M from M' by doing a surgery on a fiber which is not in V . Hence we have a Legendrian curve with twisting number -1 in our manifold M . We can assume that the Legendrian ruling slope on $\partial(\Sigma \times S^1)_i$ for $i = 1, 2$ is ∞ . Take an annulus A_i between ∂V and $\partial(\Sigma \times S^1)_i$ for $i = 1, 2$. There might be some bypasses on $\partial(\Sigma \times S^1)_i$ by the imbalance principle (3.12). After attaching these bypasses the slope of the dividing curve on $\partial(\Sigma \times S^1)_i$ is $\lfloor \frac{q_i}{p_i} \rfloor$ for $i = 1, 2$. One can similarly prove that the dividing curve on $\partial(\Sigma \times S^1)_i$ is $\lfloor \frac{q_i}{p_i} \rfloor$ for $i = 3, 4$.

Combining tight contact structures on the basic blocks

After we glue the two $\{\text{pair of pants}\} \times S^1$ across the toric annulus we get $\{\text{shirt}\} \times S^1$ which we call Y' . The slope of the dividing curves on the boundary tori of Y' is $\lfloor \frac{q_i}{p_i} \rfloor$ for $i = 1, 2, 3, 4$. We take a suitable diffeomorphism of $\{\text{shirt}\} \times S^1$ to normalise the boundary slopes to be $\sum_{i=1}^4 \lfloor \frac{q_i}{p_i} \rfloor = s$ on one of the boundary torus and 0 on the other three boundary tori. This amounts to a section change (refer Prop2.1 in [Hat]). We denote this $\{\text{shirt}\} \times S^1$ by Y . The number of tight contact structures up to contact isotopy on the manifold before the section change is the same as the number of tight contact structures up to contact isotopy on the manifold after the section change. Since

Figure 4.22: Decomposition of Y .

$s \geq 0$ we can decompose Y in a $\{\text{shirt}\} \times S^1$ with all four boundary slopes 0 and a toric annulus with boundary slopes 0 and s . This is shown in Figure 4.22.

There are three tight contact structures with zero Giroux torsion on $\{\text{shirt}\} \times S^1$ with all four boundary slopes 0 (as proved in section 4.2.3). There are $(s + 1)$ tight contact structures on a toric annulus with boundary slopes 0 and s [Hon1]. When we glue this toric annulus on $\{\text{shirt}\} \times S^1$, we need the signs of the regions on the boundary to match. One can draw all combinations and check that amongst $3s + 3$ only $2s + 3$ are possible. So we get an upper bound of $2s + 3$ on the number of potential tight contact structures represented by dividing curves on $\{\text{shirt}\} \times S^1$.

We write the boundary slopes on Y as (s_1, s_2, s_3, s_4) where the slope s_i is $s(\partial Y)_i$. Say that our boundary slopes on Y are $(2, 0, 0, 0)$. We will show that the two dividing curve configurations shown on a shirt in Figure 4.23 (top right and top left) represent two different sections (as in Prop. 2.1 in [Hat]) of the same contact structure on $\{\text{shirt}\} \times S^1$. We start with a tight contact structure that has a positive and negative bypass on the boundary component with boundary slope 2. This dividing curve configuration is shown on the top left. Consider an annulus A between boundary component having slopes 2 and 0, as shown in Figure 4.23. We do the section change (as in Prop. 2.1 in [Hat]) across annulus A to get Y'' with boundary slopes $(1, 1, 0, 0)$. We obtain the dividing curves on the new section of Y'' as follows: we start with our old section on $\{\text{shirt}\} \times S^1$ with boundary slopes $(2, 0, 0, 0)$ and draw the dividing curves on the shirt as well as on all four boundary tori. Using the construction as in Prop. 2.1 in [Hat] we draw our new section (with boundary slopes $(1, 1, 0, 0)$) in our old $\{\text{shirt}\} \times S^1$ (with boundary slopes $(2, 0, 0, 0)$). We mark all intersections of the dividing curves with the boundary of the new section. Since the new shirt is embedded in old $\{\text{shirt}\} \times S^1$, we start drawing the dividing curve at one of the boundary components with slope 1 and follow through in our new shirt across the old section. We get the dividing curves connecting the two boundary components with boundary slopes 1. This dividing curve configuration is shown in Figure 4.23 at the bottom. Next, we look at the dividing curve configuration which has the two same signed bypasses on the boundary component with slope 2 and half a twist

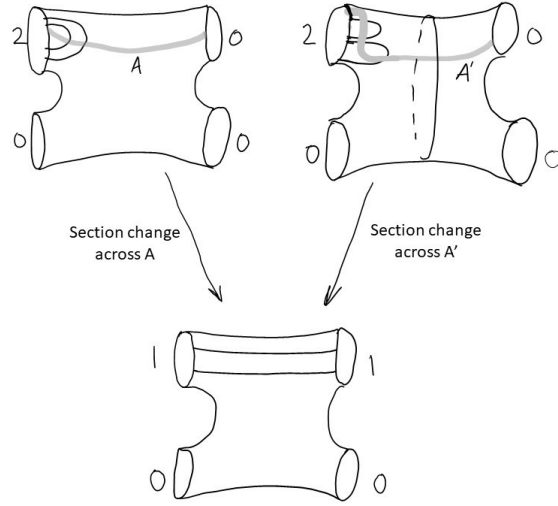


Figure 4.23: Different sections of a tight contact structures on $\{\text{shirt}\} \times S^1$.

across the incompressible torus. This dividing curve configuration is shown on the top right. We do the section change along annulus A' between boundary components having slopes 2 and 0 which goes across the half twist. We get the dividing curves (using the same process as above) connecting the two boundary components with boundary slopes 1. After the section change, we get the dividing curve configuration as shown in Figure 4.23 at the bottom. Hence one can get the top right dividing curve configuration from the top left dividing curve configuration by section change on the $\{\text{shirt}\} \times S^1$. Hence the top right and the top left dividing curve configurations are two different sections of the same tight contact structure on Y .

We had the upper bound $2s + 3$ of potential tight contact structures represented by dividing curves on $\{\text{shirt}\} \times S^1$. One can draw the dividing curves to check that s many tight structures are represented by two different sections (one with a positive and a negative bypass and the other with the same signed bypass and half a twist across the incompressible torus) in the upper bound $2s + 3$. Hence we get a tighter upper bound of $s + 3$. Since $s = \sum_{i=1}^4 \lfloor \frac{q_i}{p_i} \rfloor$ and $e_0(M) = \lfloor \frac{-q_1}{p_1} \rfloor + \lfloor \frac{-q_2}{p_2} \rfloor + \lfloor \frac{-q_3}{p_3} \rfloor + \lfloor \frac{-q_4}{p_4} \rfloor$ we get that $s + 3 = |e_0(M) + 1|$. Hence the number of the potential tight contact structures on $\{\text{shirt}\} \times S^1$ is bounded above by $|e_0(M) + 1|$.

The solid torus V_i has a boundary slope of $-\frac{q_i - \lfloor \frac{q_i}{p_i} \rfloor p_i}{v_i - \lfloor \frac{q_i}{p_i} \rfloor u_i} = -\frac{q_i + (a_0^i + 1)p_i}{v_i + (a_0^i)u_i}$. With this boundary slope, there are exactly $\prod_{j=1}^m (a_j^i + 1)$ tight contact structures on V_i (Theorem 2.3 in [Hon1]). Thus, up to contact isotopy there are at most $|(e_0(M) + 1)| \prod_{i=1}^4 \prod_{j=1}^m (a_j^i + 1)$ tight contact structures with zero Giroux torsion on $M = M(0; -q_1/p_1, -q_2/p_2, -q_3/p_3, -q_4/p_4)$ with $e_0(M) \leq -4$.

Since the upper bound and lower bound match, we get $|\pi_0(\text{Tight}^{\min}(M))| = |(e_0(M) + 1)|\prod_{i=1}^4 \prod_{j=1}^m (a_j^i + 1)$. All of these are Stein fillable since we get these contact structures on M by doing a -1 Legendrian surgery on a Legendrian link in (S^3, ξ_{std}) .

Since M is toroidal there are \mathbb{Z}^+ many non-isotopic tight contact structure on M corresponding to integral Giroux torsion. As seen in example case the tight contact structures on M with non zero Giroux torsion are not weakly fillable.

4.4 Concluding remarks

One can try to classify tight contact structures on Seifert fibred manifold $M = M(0; -q_1/p_1, -q_2/p_2, -q_3/p_3, -q_4/p_4)$ where $e_0 > -4$ and $p_i, q_i \in \mathbb{Z}$ with $p_i \geq 2, q_i \geq 1$ and $\gcd(p_i, q_i) = 1$. We can constructing tight contact structures with zero Giroux torsion by Legendrian surgery to get a lower bound on the number of tight contact structures. To get the upper bound on the number of tight contact structures we use convex surface theory. These two bounds don't match. Currently the author is unable to find any contact isotopy between the contact structures found by convex surface theory or find an invariant to say that those are non-isotopic contact structures.

Bibliography

- [B] Bennequin D. Entrelacements et équations de Pfaff (Doctoral dissertation, Université de Paris VII).
- [Col] Colin V. Sur la torsion des structures de contact tendues. In *Annales scientifiques de l'Ecole normale supérieure* 2001 (Vol. 34, No. 2, pp. 267-286).
- [CGH] Colin V, Giroux E, Honda K. On the coarse classification of tight contact structures. arXiv preprint math/0305186. 2003 May 13.
- [Eli] Eliashberg, Y., 1989. Classification of overtwisted contact structures on 3-manifolds, *Inventiones mathematicae*, 98(3), pp.623-637.
- [Eli1] Eliashberg Y. Filling by Holomorphic Discs and its Applications. *Geometry of Low-Dimensional Manifolds: Volume 2: Symplectic Manifolds and Jones-Witten Theory*. 1990;2:45.
- [Eli2] Eliashberg, Y., 1990. Topological characterization of Stein manifolds of dimension $2j$. *International Journal of Mathematics*, 1(01), pp.29-46.
- [Eli3] Eliashberg Y. Contact 3-manifolds twenty years since J. Martinet's work. In *Annales de l'institut Fourier* 1992 (Vol. 42, No. 1-2, pp. 165-192).
- [Eli4] Eliashberg Y. Legendrian and transversal knots in tight contact 3-manifolds. *Topological methods in modern mathematics* (Stony Brook, NY, 1991). 1993;171193.
- [Et1] Etnyre JB. Tight contact structures on lens spaces. *Communications in Contemporary Mathematics*. 2000 Nov;2(04):559-77.
- [EH] Etnyre JB, Honda K. On the nonexistence of tight contact structures. *Annals of Mathematics*. 2001 May 1:749-66.
- [Etn] Etnyre, J.B., 2001. Introductory lectures on contact geometry. arXiv preprint math/0111118.

- [Gay] Gay DT. Four-dimensional symplectic cobordisms containing three-handles. *Geometry & Topology*. 2006 Oct 28;10(3):1749-59.
- [Gei] Geiges H. An introduction to contact topology. Cambridge University Press; 2008 Mar 13.
- [GS] Ghiggini, P. and Schönenberger, S., 2002. On the classification of tight contact structures. arXiv preprint math/0201099.
- [GLS1] Ghiggini P, Lisca P, Stipsicz A. Classification of Tight Contact Structures on Small Seifert 3-Manifolds with. *Proceedings of the American Mathematical Society*. 2006 Mar 1:909-16.
- [GLS2] Ghiggini P, Lisca P, Stipsicz A. Tight contact structures on some small Seifert fibred 3-manifolds. *American journal of mathematics*. 2007;129(5):1403-47.
- [G] Ghiggini P. On tight contact structures with negative maximal twisting number on small Seifert manifolds. *Algebraic and Geometric Topology*. 2008 May 12;8(1):381-96.
- [GH] Ghiggini P, Honda K. Giroux torsion and twisted coefficients. arXiv preprint arXiv:0804.1568. 2008 Apr 9.
- [Gir3] Giroux E. Structures de contact en dimension trois et bifurcations des feuilletages de surfaces. arXiv preprint math/9908178. 1999 Aug 23.
- [Gir1] Giroux E. Géométrie de contact: de la dimension trois vers les dimensions supérieures. *Proceedings of the International Congress of Mathematicians, Vol. II (Beijing, 2002)*, 405–414, Higher Ed. Press, Beijing, 2002.
- [Gir2] Giroux E. Convexity in contact topology. *Comment. Math. Helv.* 1991 Jan 1;66:637-77.
- [GoS] Gompf RE, Stipsicz AI. 4-manifolds and Kirby calculus. *American Mathematical Soc.*; 1999.
- [Hat] Hatcher, A., 2007. Notes on basic 3-manifold topology. <https://pi.math.cornell.edu/hatcher/3M/3M.pdf>
- [Hon1] Honda, K., 2000 On the classification of tight contact structures I: lens spaces, solid tori, and $T^2 \times I$. *Geom. Topol.* 309-368 (electronic).
- [Hon2] Honda, K., 2000. On the classification of tight contact structures II. *Journal of Differential Geometry*, 55(1), pp.83-143.
- [HKM] Honda K, Kazez WH, Matić G. Tight contact structures and taut foliations. *Geometry and Topology*. 2000 Sep 12;4(1):219-42.

- [HKM1] Honda K, Kazez WH, Matić G. Convex decomposition theory. *International Mathematics Research Notices*. 2002 Dec;2002(2):55-88.
- [Hon] Honda K. Notes for math 599: contact geometry. Lecture Notes available at <http://www-bcf.usc.edu/~khonda/math599/notes.pdf>.
- [LM] Lisca, P. and Matić, G., 1998. Stein 4-manifolds with boundary and contact structures. *Topology and its Applications*, 88(1-2), pp.55-66.
- [LiM] Makar-Limanov S. Tight contact structures on solid tori. *Transactions of the American Mathematical Society*. 1998;350(3):1013-44.
- [LS] Lisca P, Stipsicz AI. Ozsváth-Szabó invariants and tight contact 3-manifolds, III. *Journal of Symplectic Geometry*. 2007 Dec;5(4):357-84.
- [JM] Martinet J. Formes de contact sur les variétés de dimension 3. In *Proceedings of Liverpool Singularities Symposium II 1971* (pp. 142-163). Springer, Berlin, Heidelberg.
- [Pat] Massot, P., 2014. Topological methods in 3-dimensional contact geometry. In *Contact and symplectic topology* (pp. 27-83). Springer, Cham.
- [M] Matković I. Classification of tight contact structures on small Seifert fibred L -spaces. *Algebraic and geometric topology*. 2018 Jan 10;18(1):111-52.
- [Sim] Simone J. Tight contact structures on some plumbed 3-manifolds. arXiv preprint arXiv:1710.06702. 2017 Oct 18.
- [Siv] Steven Sivek Notes on Contact Topology <http://wwwf.imperial.ac.uk/~ssivek/courses/12s-math273.php>.
- [Wan] Wand A. Tightness is preserved by Legendrian surgery. *Annals of Mathematics*. 2015 Sep 1:723-38.
- [W] Wu H. Tight contact structures on small Seifert spaces (Doctoral dissertation, Massachusetts Institute of Technology).
- [Kan] Kanda, Y., 1997. The classification of tight contact structures on the 3-torus. *Communications in Analysis and Geometry*, 5(3), pp.413-438.